

Bio-Inspired Design of Next Generation

Honeycomb Sandwich Panel Cores

by

Derek Lee Goss

A Thesis Presented in Partial Fulfillment  
of the Requirements for the Degree  
Master of Science

Approved April 2020 by the  
Graduate Supervisory Committee:

Dhruv Bhate, Chair  
Sharon Lewis  
Changho Nam

ARIZONA STATE UNIVERSITY

May 2020

## ABSTRACT

Honeycomb sandwich panels have been used in structural applications for several decades in various industries. While these panels are lightweight and rigid, their design has not evolved much due to constraints imposed by available manufacturing processes and remain primarily two-dimensional extrusions sandwiched between facings. With the growth in Additive Manufacturing, more complex geometries can now be produced, and advanced design techniques can be implemented into end use parts to obtain further reductions in weight, as well as enable greater multi-functionality. The question therefore is: how best to revisit the design of these honeycomb panels to obtain these benefits?

In this work, a Bio-Inspired Design approach was taken to answer this question, primarily since the hexagonal lattice is so commonly found in wasp and bee nests, including the well-known bee's honeycomb that inspired these panel designs to begin with. Whereas prior honeycomb panel design has primarily focused on the hexagonal shape of the unit cell, in this work we examine the relationship between the various parameters constituting the hexagonal cell itself, specifically the wall thickness and the corner radius, and also examine out-of-plane features that have not been previously translated into panel design. This work reports findings from a study of insect nests across 70 species using 2D and 3D measurements with optical microscopy and X-ray tomography, respectively. Data from these biological nests were used to identify design parameters of interest, which were then translated into design principles. These design principles were implemented in the design of honeycomb panels manufactured with the Selective Laser Sintering process and subjected to experimental testing to study their effects on the mechanical behavior of these panels.

## ACKNOWLEDGMENTS

This work was funded by the National Aeronautics and Space Administration (NASA) STTR program under contract 80NSSC18P2131 in support of the PeTaL (Periodic Table of Life) project. Dr. Vikram Shyam is the Principal Investigator for PeTaL.

I would like to first thank Cameron Noe and Christine Lee for helping with creating samples and specimens that allowed this work to be carried out. Next on the biology side of this project, Clint Penick who coordinated with the American Museum of Natural History to allow us to collect our wasp nest data as well as working with the phylogenetic aspects of the data. From AMNH I would like to thank Christine Lebeau, she was very open and helpful during our time in her facility. Finally, my advisor Dr. Dhruv Bhate. I have worked with him for two years now and he has always encouraged my work and pushed me to make it as meaningful as I could. I would also like to acknowledge support from NASA, who supported me, and this work in the form of a Space Grant Fellowship, and an STTR Phase I award.

## TABLE OF CONTENTS

	Page
LIST OF TABLES.....	x
LIST OF FIGURES.....	v
CHAPTER	
1 INTRODUCTION .....	1
Section 1.....	3
Section 2.....	4
2 A COMPARATIVE STUDY OF INSECT NESTS.....	6
Section 1 .....	6
Section 2 .....	12
Section 3.....	21
3 BIO-INSPIRED DESIGN PRINCIPLES.....	27
Section 1 .....	27
Section 2 .....	31
4 ADDITIVE MANUFACTURING OF HONEYCOMB CORE .....	41
Section 1 .....	41
5 MECHANICAL BEHAVIOR .....	46
Section 1 .....	46
Section 2.....	50
6 Open Questions .....	51
REFERENCES .....	52

## LIST OF TABLES

Table		Page
1.	Thesis Objectives .....	5
2.	Insect Nest Data Break Down .....	22
3.	Specimen Modeling Steps .....	43
4.	Full Factorial DOE .....	44

## LIST OF FIGURES

Figure		Page
1.	Bullet Train Modeled After Kingfisher Beak .....	1
2.	Natural Honeycomb vs Honeycomb Sandwich Panel .....	3
3.	Sample of Hymenoptera Phylogeny .....	7
4.	Parameter Measurement Examples .....	8
5.	Wax Wall Thickness Over Time .....	8
6.	Honeycomb Examples .....	9
7.	Hive and Frame Labels .....	10
8.	American Museum of Natural History .....	10
9.	Wasp Nest Example .....	11
10.	Two Cell Wide Nest .....	12
11.	Keyence VR 3200 .....	13
12.	Single Cell Scans of <i>Apoica flayissima</i> .....	14
13.	Optical vs Height Scan Data .....	14
14.	Insect Nests Profile .....	15
15.	Edge Detection in Keyence Analyzer .....	16
16.	Measurement Within Keyence Analyzer .....	16
17.	Unique Fixturing Require per Sample .....	17
18.	Domed Wasp Nest Cells .....	18
19.	Crushed Wasp Nest .....	18
20.	All Dimensions Taken From a Single Cell .....	19
21.	Micro CT X-ray Generation .....	20
22.	Micro CT Sample .....	21
23.	Insect Nest Database .....	22
24.	Coner Radius vs Cell Diameter .....	23

Figure	Page
25. Wall Thickness vs Cell Diameter .....	24
26. Paper Type Definition .....	24
27. Corner Radius Normalized by Cell Radius .....	25
28. Wall Thickness Normalized by Cell Diameter .....	26
29. Compression Testing of Corner Radius Variation .....	28
30. ANSYS Parameter Optimization .....	29
31. Cell Coping .....	30
32. Cell Wall Thickness Study .....	31
33. Wall Thickness by Slice Number .....	32
34. Walls of Cells And Interface .....	33
35. Opposing Walls of Cells .....	33
36. Micro CT of Cell Interface .....	34
37. Cell Wall Termination .....	35
38. Cell Interface Sample .....	35
39. Cross Section of Single Cell .....	38
40. Complex Internal Geometry Example .....	46
41. SLS Printing Process .....	47
42. SLS Powder Removal Steps .....	48
43. Bending and Compression Samples .....	49
44. Instron 5985 250kN Load Frame .....	51
45. Compression Platens with Sample .....	52
46. Three-point Bend Fixture with Sample .....	54
47. Compression Calculations .....	55
48. Load vs Displacement: Traditional Samples .....	56

Figure		Page
49.	Load vs Displacement: 30-Degree Samples .....	56
50.	Load vs Displacement: 45-Degree Samples .....	57
51.	Load vs Displacement: 60-Degree Samples .....	57
52.	Energy Density Versus Specific Modulus .....	58
53.	Modulus of Elasticity vs Varied Parameters .....	59
54.	First Maximum Stress vs Varied Parameters.....	60
55.	Energy Absorbed vs Varied Parameters .....	61
56.	Three-Point Bend Raw Data .....	62
57.	Flexural Rigidity Analysis .....	63
58.	Maximum Flexural Stress Analysis .....	64
59.	Equations For Three-Point Bend Data .....	65



## CHAPTER 1

### INTRODUCTION

As societies and populations continue to evolve, engineers and designers are constantly facing new problems with how best to advance current technologies and engineering techniques to meet the world's needs. Aircraft need to fly faster and farther while weighing less than they do now, cities need to hold more people while using less materials and having less of an impact on the environment, structures need to be able to perform more than one function at a time at various scales, and list goes on. In the past, these engineers and designers have come up with solutions they believe will address their current issue, test it, redesign and repeat until they have a design that meets their specifications. This process has been used for centuries and has led to every great technological breakthrough humans have known. But this process takes time and resources, time that could be spent working on another problem and resources that could be put to multiple challenges. So, the question arises; is there a way to jump the line so to speak, and reach a final solution quicker?

This is where nature can come to the aid of these engineers and designers. Nature has had plenty of time to identify its own unique set of challenges and even more time to try to solve them [1], [2]. By observing and learning how nature addresses certain design challenges, an individual trying to solve a similar problem now has a reference point to start from rather than starting from the very beginning. History is full of advancements and techniques that have built off those that came before it in some form or another. With nature, engineers and designers now have hundreds of thousands of environments, loading conditions, materials, multi-functional structures, and multiple variations of each to observe and learn from.



Figure 1: Bullet train modeled after Kingfisher beak [3]

Figure 1 shows an example of a bullet train modeled after the beak of the Kingfisher. The Kingfisher uses its beak to dive through water in order to catch fish, its beak needs to be able to cut through the water without disturbing the prey below. By studying how nature has solved the problem of gliding through a liquid with minimal resistance, designers were able to mimic this for a structure that needs to glide through the air [3]. There are many examples in literature and the mainstream media of natural design being leveraged to solve an engineering problem, this example however is different from most. The 500 Series Shinkansen bullet train was able to travel faster and created less ambient noise in the process to disturb its urban surroundings; this new design now has a multifunctional purpose. Multifunctional structures, at any scale, are plentiful in nature but have proven to be difficult to design through traditional means. Organisms in nature rarely have one problem to solve as they evolve, most must perform multiple functions even at the same time. Engineering challenges arise often that can benefit from multifunctionality. If a lattice structure could be constructed for the wing of an aircraft that can reduce weight can also draw heat away from the engine, the performance of the entire structure increases.

Another classic example of an engineering challenge using natural design to solve, is that of the honeycomb. Honeycomb has drawn the attention of mathematicians, biologists and engineers since the time of the Romans [4], [5]. Exactly how bees create these hexagonal lattices still remains a mystery to this day but is an example of nature using a structure for multiple purposes. Bee honeycomb holds not only bees but their larva, honey and the pollen needed to create the honey. As honey is created and consumed, the weight it imposes on the structure changes through a year, creating a slow, but cyclical loading condition. This comb must also be strong enough to resist a gust of wind from bending it far enough to detach from a tree or whatever it was built of off.

### 1.1 Research Questions

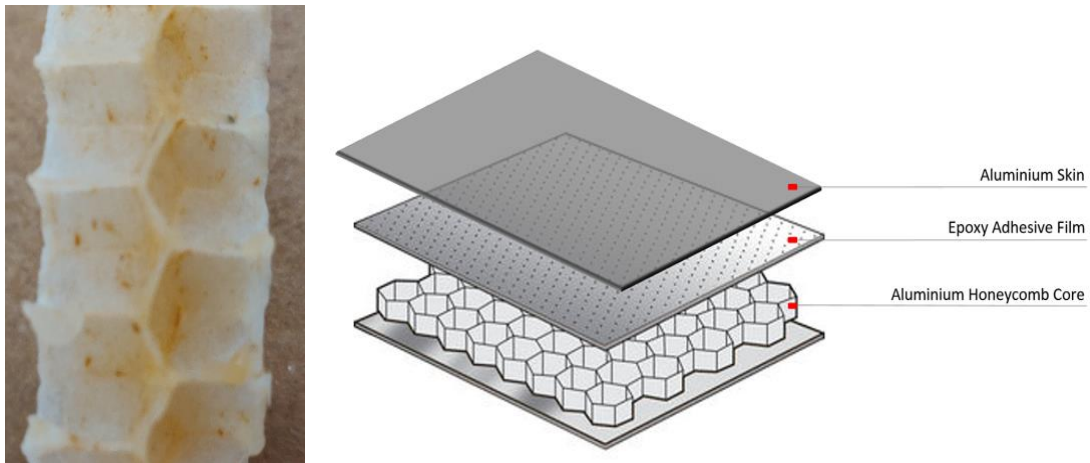


Figure 2: Natural honeycomb vs a honeycomb sandwich panel

The idea of using this hexagonal lattice is not a novel concept, however. A patent was first filed for using this design in the early 1900's and has been used in applications requiring high stiffness and low weight ever since [6], [7]. Honeycomb panels find their use in aerospace applications where weight saving is key component to a vehicle's success. Current honeycomb used in these applications is a highly idealized version of what can be found in nature. For example, as can be seen in

Figure 2, natural honeycomb is not made of a single wall of cells open at either side. Cells have a corner radius rather than a sharp corner. The previous statement is not meant to discount the usefulness of the current design, it is meant to ask questions:

- Can the current design be improved upon?
- Can a closer study of natural honeycomb lead to a design with improved mechanical properties such as stiffness and strength?

More questions that arise when looking at nature.:

- How do parameters within natural specimens relate to one another?
- Does the material of the specimen matter for the relation of parameters?
- What patterns arise from these parameters?

## 1.2 Thesis Objectives

This thesis will attempt to investigate and answer the research questions laid out above. The two parts of this study are as follows: a comparative study of honeybee and wasp nest geometry, and the biomimetic design of next generation honeycomb sandwich panels. The first half of this work describe a study conducted on insect nests aimed at identifying relationships between geometric parameters within samples of different material compositions. The second half is the design of honeycomb panel core based on observations and insights gained from the insect nest study. Below is a table of project objectives and how they were undertaken.

Objective	Test / Research
Parameterization of insect nests	Literature review and observation
Data collection of parameters	Digitization of insect nests <ul style="list-style-type: none"> <li>• White light microscopy</li> <li>• Micro CT</li> </ul>
Data Analysis	<ul style="list-style-type: none"> <li>• Plotting data sets from digitization</li> <li>• Conducting statistical analysis on data sets</li> </ul>
Design test specimen based on insect nest parameters	CAD modeling of idealized honeycomb core
Study effect of parameters on mechanical behavior	Conduct mechanical testing of previously designed specimen
Data Analysis	<ul style="list-style-type: none"> <li>• Plotting data sets from testing</li> <li>• Conducting statistical analysis on data sets</li> </ul>

Table 1: Thesis objectives

## CHAPTER 2

### A COMPARATIVE STUDY OF INSECT NESTS

This section begins by discussing the collection of insect nests across seventy separate species of the Hymenoptera order. Next, key parameters of the structures are defined and measured using primarily structure white light scanning. After these parameters have been measured, statistical analysis of their relation to one another and to the building material was conducted.

#### 2.1 Specimen Collection

Specimens collected for this study came from the Hymenoptera order of insects, which contains sawflies, bees, wasps and ants [8], [9]. Within this order, only bee and wasp nests were gathered and analyzed because these subcategories are among the only members that produce hexagonal cells within their nests. Not all bees and wasps produce hexagonal cells those that do not were excluded from this study. With just hexagonal cells in mind, another variable comes into play; the materials these nests are constructed from. When looking at bee species that produce hexagonal cells, it can be observed that wax is the only material used for construction. In the case of wasps, it can be observed that paper, wax, and in some cases a combination of the two are used for nest construction, as observed in the Phylogeny demonstrated in Figure 3.

	Subfamily	Members	Nest material	Usage	Image	Environment
	Polistinae	<i>Polistes dominula</i>	Paper	Brood rearing		Temperate/tropical
	Vespinae	<i>Dolichovespula maculata</i>	Paper	Brood rearing		Temperate/tropical
	Stenogastrinae	<i>Liostenogaster flavolineata</i>	Mud	Brood rearing		Tropical
	Apinae	<i>Apis dorsata</i> <i>Apis florea</i> <i>Apis mellifera</i>	Wax	Brood rearing Nectar storage Pollen storage		Temperate/tropical

Figure 3: Phylogenetic relationships among wasp and bee species with different materials (courtesy Clint Penick)

With these constraints on which nests could be looked at that contain hexagonal cells, the next step in gathering samples was determining what construction material were of interest. An initial literature review showed that certain cell parameters, wall thickness and cell diameter, varied from not only from the different building materials but also from species to species. At the conclusion of this review, it was determined that each of the three primary materials would be analyzed and multiple species using the same material would be analyzed if available. In Figure 4, we can see the three key parameters that is work will measure and analyze: wall thickness, cell diameter and corner radius. These three parameters define the hexagonal lattice and can be seen to vary depending on material and species.



Figure 4: Parameter measurement examples

### 2.1.1 ASU Bee Lab Nest Creation

Amongst different bee species, there is a measurable difference in cell size depending on the size of the bee creating each of the nests. With this in mind, locating nests from different species was evaluated and eventually ruled out as a possibility for this study. Two species that were of interest were *Apis florea* (dwarf honeybee) and *Apis dorsata* (giant honeybee), unfortunately these species are both located in South and Southeast Asia. Rather than traveling to these locations to measure nests, the option of importing them into the country arose. However, there is currently a ban on the import of natural honeycomb from fear of spreading disease to native species. Another factor that must be mentioned when discussing measuring bee's wax is how old the comb is relative to when it is measured. As these combs age, they gather particulates and more wax and increase in size, see Figure 5.

#### **Wall Thickness**

Source	Species	Details	Thickness (mm)
Von Frisch (1974), Dadant (1975)	<i>A. m. ligustica</i> (Italian bee)	Fresh comb	0.073 ± 0.002
Zhang et al. (2010)	<i>A. m. ligustica</i> (Italian bee)	Fresh comb	0.088 ± 0.010
		Five-month old	0.120 ± 0.011
		One-year old	0.246 ± 0.030
		Two-year old	0.297 ± 0.048

Figure 5: Wax wall thickness over time, from literature [10][11]



As studying how the wall thickness varies through time is not a factor of this research, the decision was made to locate “fresh” comb that did not need to be imported in the country and preferably not into the state. The ASU School of Life Sciences – Bee Laboratory is located on the Polytechnic campus and is home to hundreds of thousands of bees constantly creating and living in wax nests. This was the obvious place for this research to partner with in order to gather wax specimens. With the lab so close and the researchers being very interested in current study, the option to have comb created specifically for this study. Instead of having estimates on when each nest was created, the opportunity to be able to know to the day how old each sample was now available.

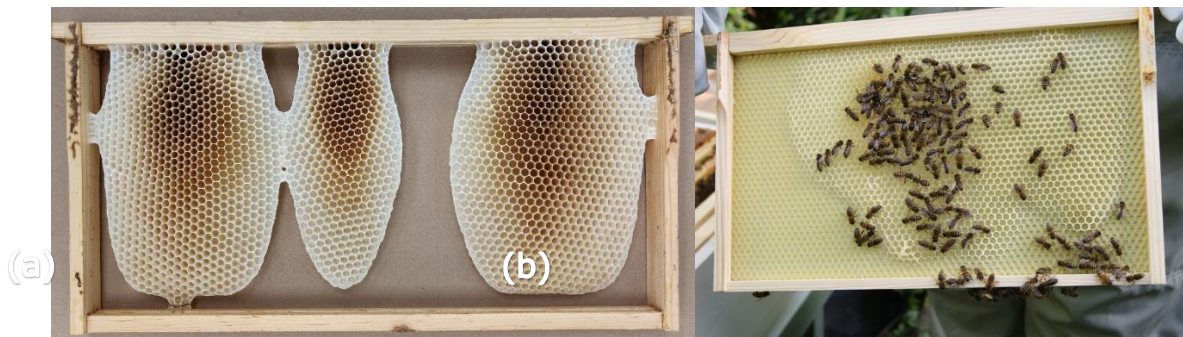


Figure 6: (a) Live frame comb and (b) comb on foundation

Fifteen individual nests were created in a “live frame” environment, see Figure 6(a), to more accurately mimic conditions the bees would experience in the wild while creating nests. Traditionally when creating new comb, beekeepers and researchers use a plastic or wax foundation to encourage the bees to produce nests faster, see Figure 6(b). This foundation influences the end result of the cell geometry and is not a fair representation of how these structures are made in the wild. The most accurate data for this study would be to find truly wild comb as it starts to be

built and monitor it until the comb was complete. This was unrealistic for this type of study and natural conditions were replicated as to introduce as little bias as possible into the specimens. See Figure 7 for an example of labeled frames.



Figure 7: Hive and frame labels

### 2.1.2 American Museum of Natural History Wasp Collection



Figure 8: American Museum of Natural History

Unlike the honeybee, wasps use two different classes of materials when constructing their nests, mud and paper. In order to analyze if this material difference plays a part in the structure of the nests, both need to be measured and compared to one another as well as being compared to nests made from wax.

Locating specimen for this side of the study was not as convenient as having the Bee Laboratory next door. After investigating wasp nest collections in the United States, the American Museum of Natural History (AMNH) in New York was identified as a potential source of nests for study [12]. AMNH does not have the largest wasp nest collection in the world but they do have the most diverse collection.

Along with the extensive collection of wasp nests, a database of information was available for each specimen. This data base included when the specimen was collected, who collected it, where it was found, as well as the taxonomy. After communicating with both AMNH and ASU Packing Services, the labs scanning white light optical microscope, which will be discussed later in this work, was shipped to New York in order to scan their specimens. Upon arriving at the AMNH facility, one thing was made clear by both the collection curators and the samples themselves, most samples were very delicate, see Figures 9 and 10, and none could be physically manipulated or damaged in anyway.



Figure 9: Wasp nest in AMNH box



Figure 10: Two cell wide nest at AMNH

## 2.2 Measurement Methods and Data Collection

In this section, several topics will be discussed for three measurement methods: data collection, challenges in data collection, and the usefulness of each method. The first piece of equipment that will be discussed will be the Keyence VR 3200, see Figure 11, this was used for the bulk of scanning and measuring in this study. Primarily two-dimensional data can be obtained using the Keyence; however, this equipment does have the ability to report some three-dimensional data depending on how a specimen is fixtured and how complex the geometry is. The following techniques, Micro Computed Tomography (Micro CT) and silicon molds were used to try to represent these nests in three dimensions. Micro CT is far more accurate for capturing data in three dimensions and has a far less chance of damaging the specimens unlike the mold making process. Creating these molds was the first attempt at capturing three-dimensional data before Micro CT was available.

### 2.2.1 Keyence VR 3200

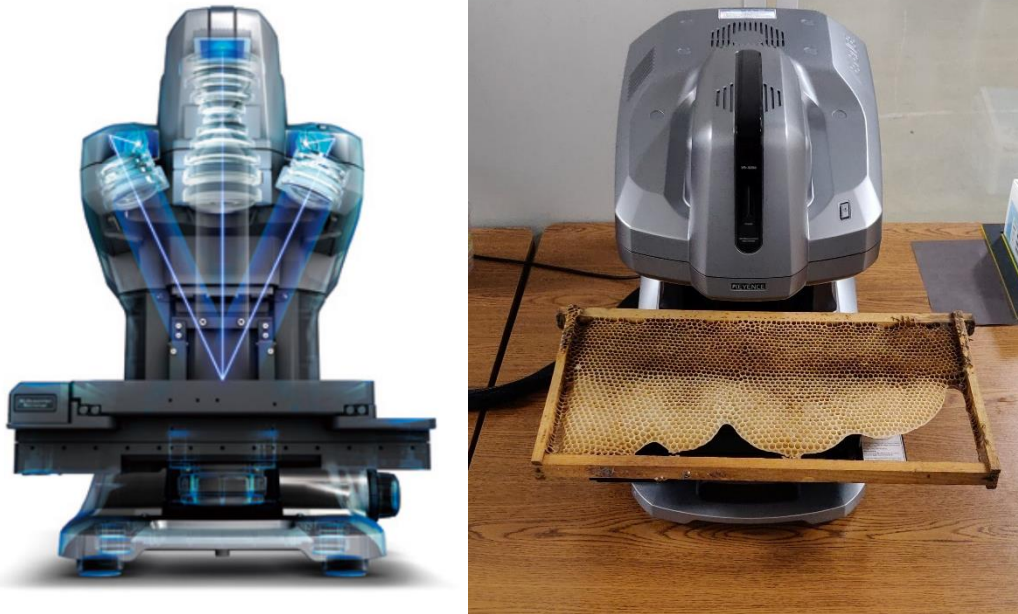


Figure 11: Keyence VR 3200

The Keyence VR 3200 was chosen to take the bulk of the measurement data for this study for several reasons; there was ready access to the equipment at most times through the study, scanning of specimens can be automated to a certain extent and the post processing analysis software that pairs with the scanner has built in edge detection for measurements.

One of the main uses of the Keyence in industrial as well as research applications is that of validation and quality control. With this goal in mind, the Keyence was designed to be able to capture data quickly but have the ability to scale to different sample and feature sizes. Single frame scans can take as little as five to eight seconds to receive data, but multiple frames can be stitched together in order to scan larger areas at once. As no two insect nests are quite the same, having this flexibility in a measurement tool was crucial for this study. Individual cells were scanned during the course of this study, see Figure 12, and an operating

magnification of 40x, some cells are too large to be captured in one frame. Having the ability to stitch together four to nine images to capture single cells allowed the data collection process to continue at a rapid rate with each scan taking on average thirty seconds.

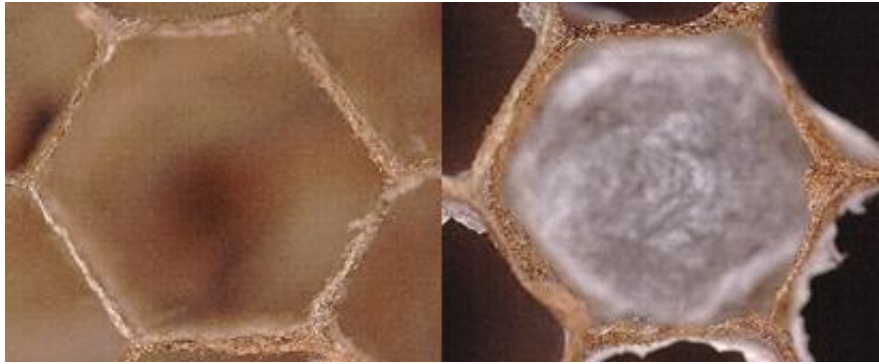


Figure 12: Single cell scans of *Apoica flavissima*

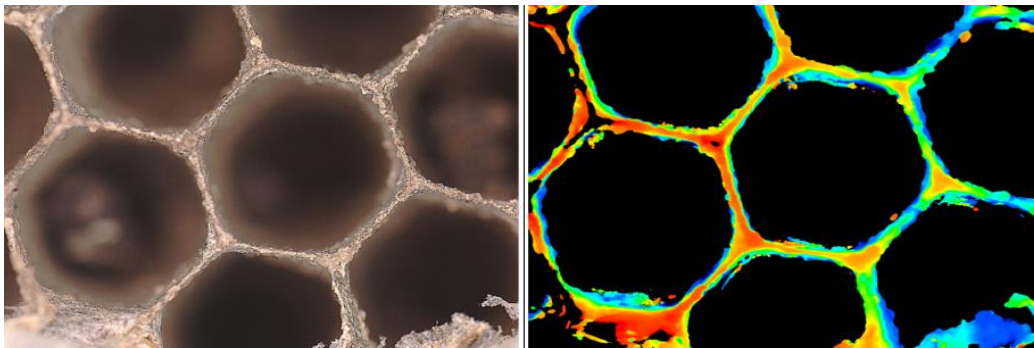


Figure 13: Optical vs height data from Keyence scans

Within the average thirty seconds it takes to scan a specimen, the Keyence is able to capture optical and height data. Optical data can be thought of as a simple photograph taken of a sample while height data is rough three-dimensional representation of the sample. As this data collection was primarily focused the on two-dimensional features of insect nests, height data was not of interest at first. Data collection using the Keyence started with scanning honeycomb from the ASU Bee Lab and as seen in Figure 14(a), the top surface, or the surface being scanned,

is relatively uniform and smooth. Without major defects or features at multiple heights, optical data for measurements gives consistent and accurate results. However, looking at an example of a wasp nest, see Figure 14(b), it can be noted that the top surface is far more uneven with even more defects. The difference between these types of nests can be attributed to the material properties of wax, paper, and subsequently mud. When wax is manipulated or a force is applied to it, there is give to the material, wax is soft and malleable. With paper, as a force is applied, the material rips, leaving jagged edges. Mud, being much more brittle than the other two materials, snaps or fractures, also leaving jagged edges.

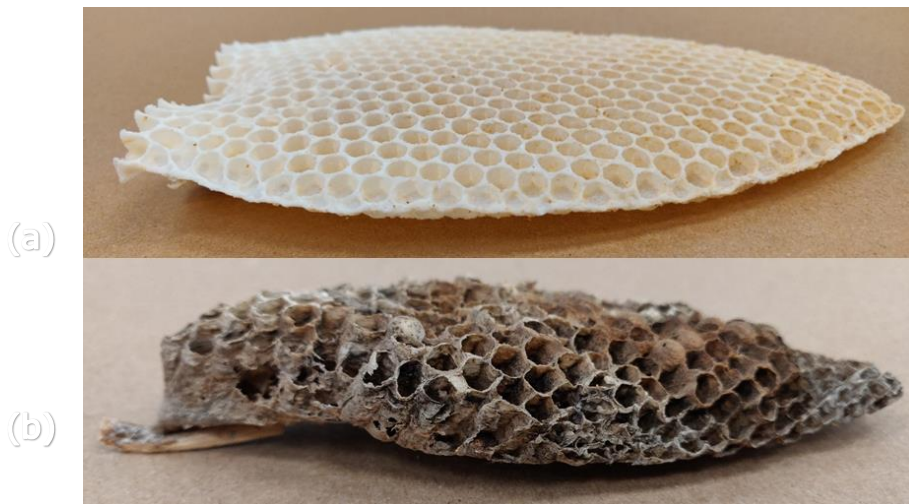


Figure 14: (a) Honeycomb profile and (b) wasp nest profile

Within the analyzing software from Keyence, the choice can be made to use either optical or height data for measurements. In some cases, using the available optical data for edge detection leads to errors in finding an edge or even incorrect detection. Edge detection relies on the user defining where the boundary of specimen is with a box, see Figure 15, the software then finds an edge within said box and creates a line or arc that best fits the given data. These edges must be defined for measurements to be taken from scan data. Edges are reference points within the

data for measurements to be attached to, see Figure 16 for a measurement example. For optical data, edge detection looks at the difference in contrast between pixels in the user defined box. If the contrast is not significant enough or there is missing data from a scan, edge detection can fail. With the ability to use height data instead, rough surfaces that can cause missing optical data can now be captured and used for edge detection. While these two options usually end in "good" data for the analyzer to use, in some cases this is not enough for edge detection to work properly. Sometimes scans must be re-done, and samples must be re-fixtured in order to correct this.

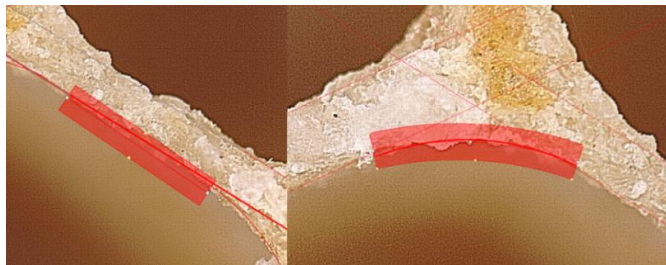


Figure 15: Edge detection in Keyence Analyzer

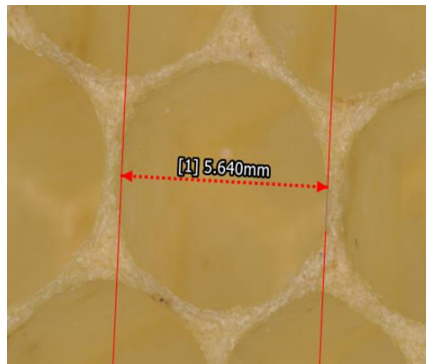


Figure 16: Measurement within Keyence Analyzer

After observing a sample like that in Figure 14(b), it can be noted that many cells within the nest are not facing the same direction as opposed to the honeycomb in Figure 14(a). In order to properly scan the top of each cell, the insect nests must be oriented in such a way that the top of the cell is parallel to the lens of the



Keyence, see Figure 17. In most cases, this did not occur only once per nest but rather per cell. As stated before, scanning only took on average thirty seconds, the vast majority of time spend gather data came from fixturing and re-fixturing each sample until all of the desired cells where captured. While collecting data for this study, it was attempted to scan at least eight cells per nest in order to maximize data per species. However, this was not always possible. Some nests had to many damaged or capped cells, see Figure 18 and 19, and some did not have eight cells in total.

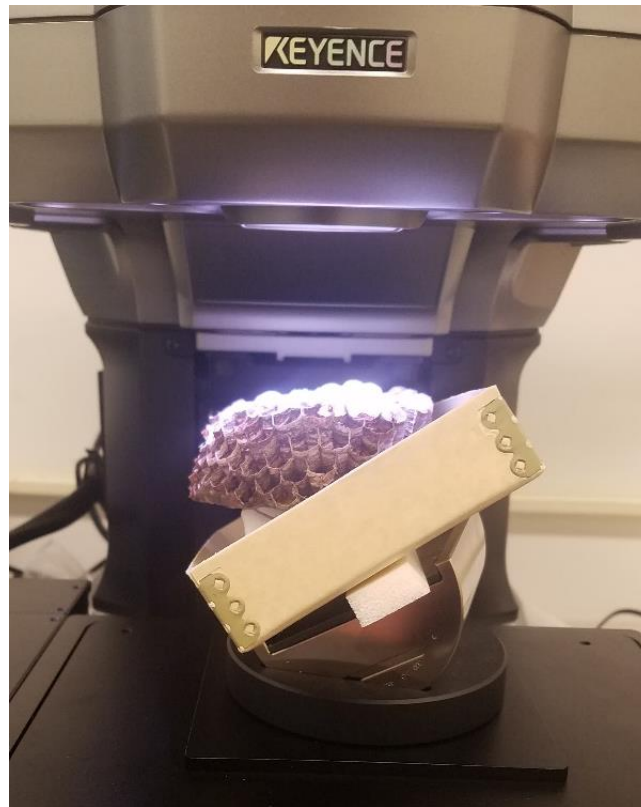


Figure 17: Unique fixturing require per sample



Figure 18: Domed wasp nest cells

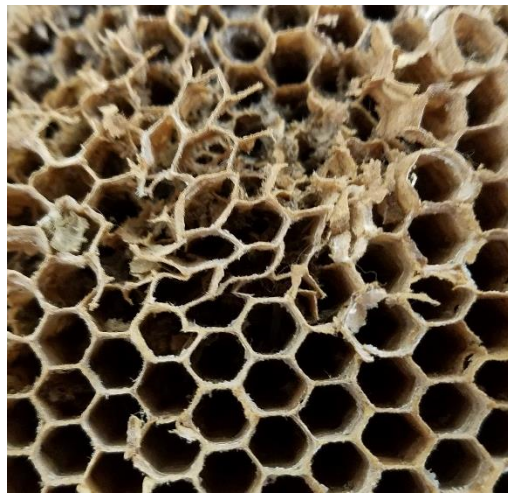


Figure 19: Crushed wasp nest

With scan data that edge detection works with, fifteen dimensions are taken from each cell. Wall thicknesses are taken from each of the six walls and corner radius is taken from all six corners. Cell diameter as measured as the distance between opposing walls, this gives three dimensions per cell. These three dimensions are averaged together for a single cell diameter value. Figure 20 shows a single cell with the fifteen dimensions imposed on top of optical scan data.

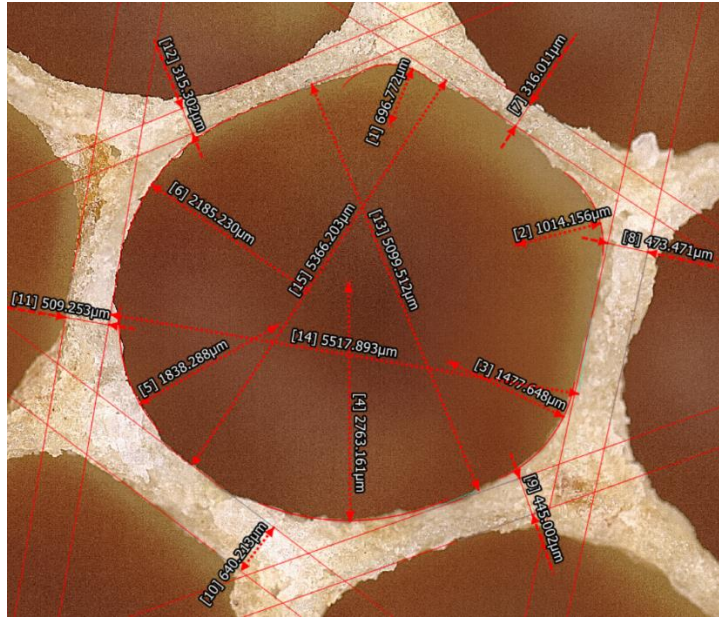


Figure 20: All dimensions taken from a single cell

### 2.2.2 Micro Computed Tomography

Micro Computed Tomography or Micro CT, Figure 21, is a form of three-dimensional imaging that uses X-ray transmission to penetrate a sample [13]. As X-rays are emitted within the system, they pass through what every sample has been placed in front of them. A detector sits on the other side of the sample, collecting the X-rays. The Micro CT passes these X-rays through samples affixed to a rotating base and calculates the density of samples based on the strength of the X-rays collected by the detector. By utilizing X-rays to map a three-dimensional object, the sample does not need to be cut apart or altered in order to characterize its internal structure. Micro CT can also report the different densities within a sample, this has been used to characterize grain structures within metals in other studies. For this study, a sample of honeycomb was scanned with honey still inside of some cells. Being able to delineate densities allowed just the wax structure to be studied.

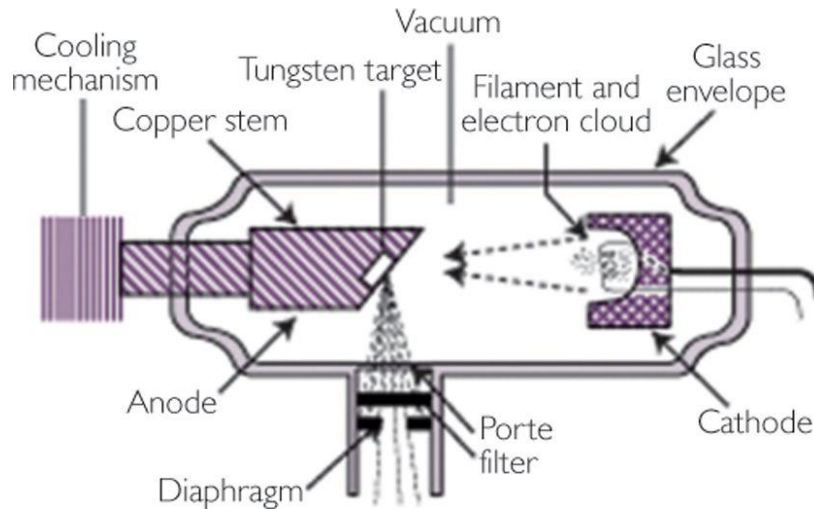


Figure 21: Micro CT X-ray generation [13]

To better understand the cell interface and coping, two features that will be discussed in the section to follow, Micro CT was leveraged. A small sample of comb was cut from a larger lobe, see Figure 22 (and fixtured within the machine and operated the machine for the scanning process. Test scans are conducted with each sample to fine tune the strength and power of the X-rays being emitted depending on the density of the part. With the parameters set for scanning the honeycomb sample, the entirety of the scan was allowed to run. Even with a sample size of roughly one inch cubed, scanning took roughly twelve hours to complete. While the information gained from the scan was insightful, the long scan times and subsequent expensive cost of the samples let the research to focus more on the structured white light scanned described previously. What else that could be done with this scanning technology will be discussed in the future work section.

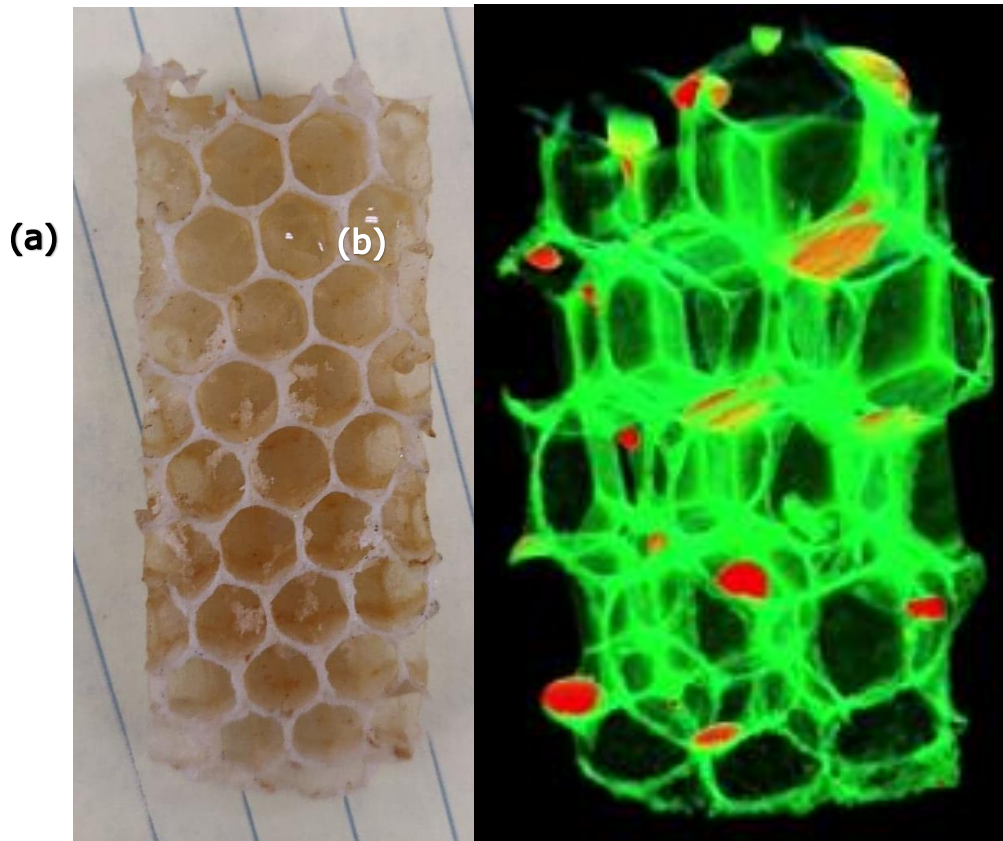


Figure 22: (a) Micro CT sample and (b) rendered model of scan

### 2.3 Data Analysis

From the measurement data gathered from both the ASU Bee Lab and AMNH, a total of seventy species and eighty-seven nests were observed. Table 2 contains the total number of nests, cells, and species per material that have been scanned and measured. A database, see Figure 23, was created to track the data from each observed cell. Each row within the database contains measurement, phylogenetic, environmental, and geographic data. Much of the non-measurement data has been taken from a data base created by AMNH to track their collection. The extra data was collected for future work to see how and if environment affects different aspects of insect nest, whether it be material or geometric properties.

	Beeswax	Mud	Paper	Paper/ Mud	Total
Number of Nests	15	2	63	7	87
Number of Cells	187	8	216	29	440
Number of Species	1	2	60	7	70

Table 2: Insect nest data breakdown

<b>Number</b>	<b>Wall thickness/Diameter</b>
<b>Nest_number</b>	<b>Corner radius/half diameter</b>
<b>AMNH_Number</b>	<b>Drone vs Worker</b>
<b>Order</b>	<b>Fiber_length</b>
<b>Family</b>	<b>Nest material</b>
<b>Subfamily</b>	<b>Collection_date</b>
<b>Tribe</b>	<b>Collection_location</b>
<b>Genus</b>	<b>Latitude</b>
<b>Species</b>	<b>Longitude</b>
<b>Species_DerekNotes</b>	<b>Elevation_m</b>
<b>Genus_species</b>	<b>Biome</b>
<b>Nest Sample</b>	<b>Collector</b>
<b>Frame Number</b>	<b>Determined_by</b>
<b>Cell Number</b>	<b>Material</b>
<b>Cell Group</b>	<b>Brittleness</b>
<b>Average Corner Radius (µm)</b>	<b>Envelope</b>
<b>Average Wall Thickness (µm)</b>	<b>Orientation (Horizontal/Vertical)</b>
<b>Average Cell Diameter (µm)</b>	<b>Swarm Founded v. Individual</b>

Figure 23: Insect nest database

With this data base laid out and complete, this data was then entered into JMP 14 for statistical analysis and plotting. As a reminder, the scope of this study was to look at how cell parameters related to one another and to investigate if nest material had effect as well. All parameters other than geometric and material, are left out from analysis at this point. Statistical relations and plots are described below.

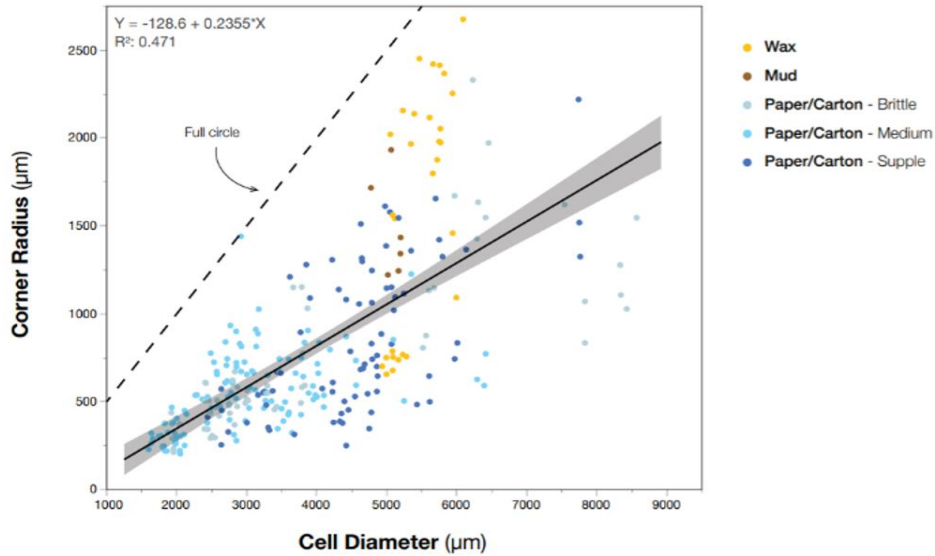


Figure 24: Corner Radius vs Cell Diameter

Figure 24 shows a plot of corner radius as a function of cell diameter with the material of each data point depicted with a different color. By looking at the material legend, it can be observed that there is more than one type of paper being plotted. The definition of these different types has been defined by a 1998 paper authored by Wenzel, see Figure 26 [8]. As previously mentioned, samples from AMNH could not be altered or damaged, a literature review was done to determine which of the species in this study use what type of paper for their nesting material. This plot also shows a line depicting where a data point needs to lay to have a parameter ratio equal to a circle. From this plot a clear trend can be seen, across all materials, as cell diameter increases, so does corner radius. On average, paper cells are smaller in size than either wax or mud. Also, where paper and wax cells reach similar cell diameters, the wax cells have a greater corner radius. With a  $R^2$  value of 0.471 it can be noted that these parameters are not perfectly linear to on another, though this can at least partially be attributed to the fact that different materials are being plotted on the same graph here.

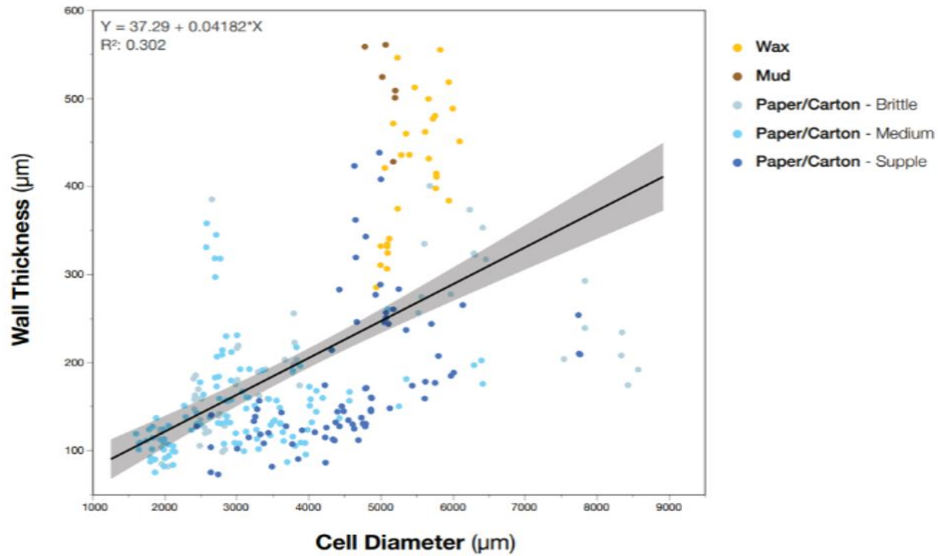


Figure 25: Wall Thickness vs Cell Diameter

Figure 25 shows a plot of wall thickness as a function of cell diameter with the material of each data point depicted with a different color. Much like the last plot, it can be observed that as cell diameter increases, so does wall thickness. When looking at cells with similar cell diameters, wax and mud cells have a much higher wall thickness as compared to the paper. With regard to paper, the three types have similar ratios of wall thickness to diameter. With a  $R^2$  value of 0.302 it can be noted that these parameters are not perfectly linear to one another.

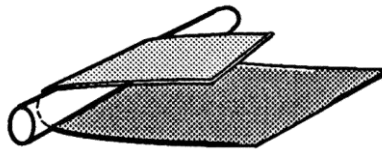


Fig. 1. Supple paper, rolled around a pencil without breaking into separate pieces.

Figure 26: Paper type definition, following Wenzel (1998) [8]



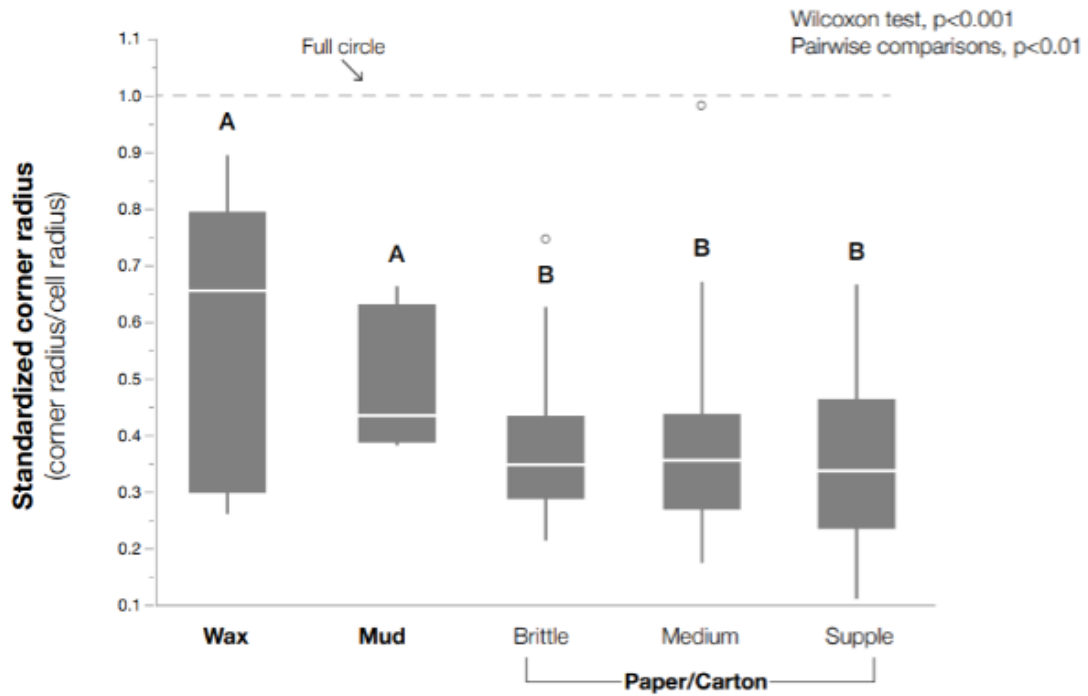


Figure 27: Corner Radius normalized by Cell Radius

Figure 27 depicts a box and whisker plot of corner radius normalized by cell radius in relation to material. This normalization is necessary to study how corner radius and wall thickness are affected by material rather than cell size. These plots show this ratio of radii is largest for wax and very similar for all three paper types. Despite different distributions of ratios, mud and wax are statistically identical while all three paper types are statistically identical to one another.

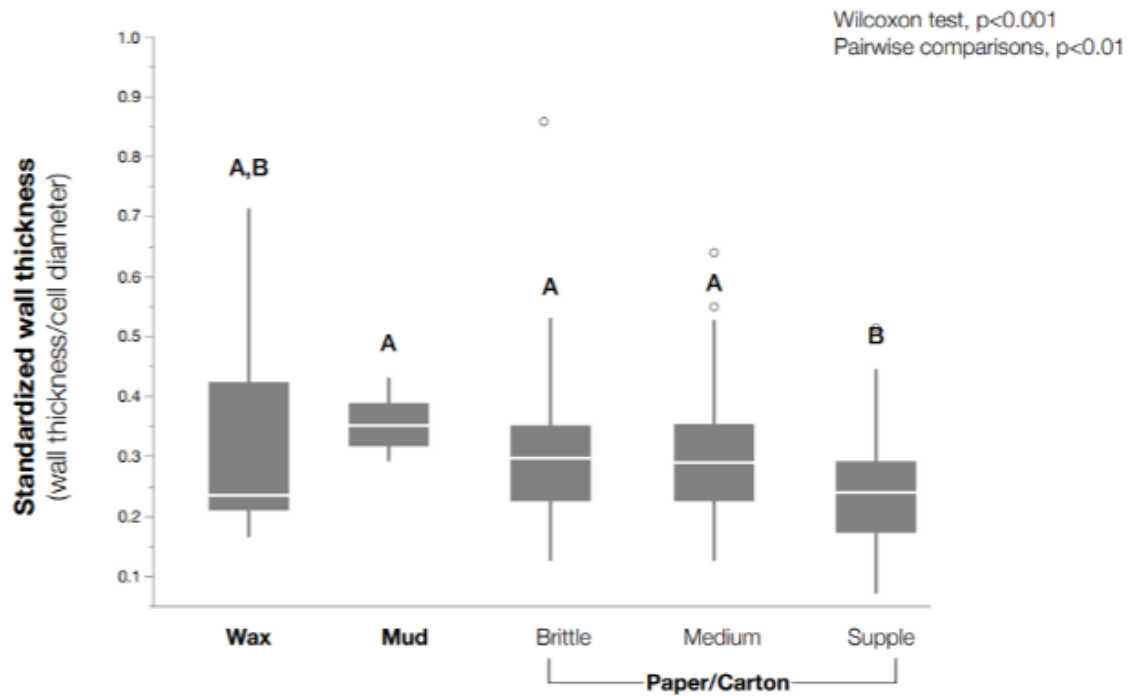


Figure 28: Wall Thickness normalized by Cell Diameter

Figure 28 depicts a box and whisker plot of wall thickness normalized by cell radius in relation to material. These plots show this ratio is largest for mud and very similar for all three paper types. Despite different distributions of ratios, mud, wax, brittle paper and medium paper are all statistically identical. Supple paper and wax are also statistically identical.

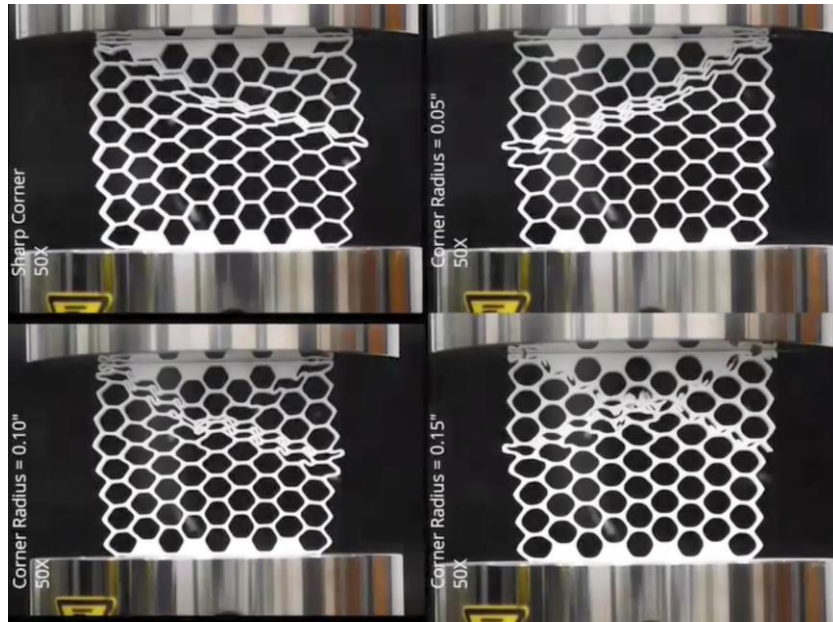
## CHAPTER 3

### BIO-INSPIRED DESIGN PRINCIPLES

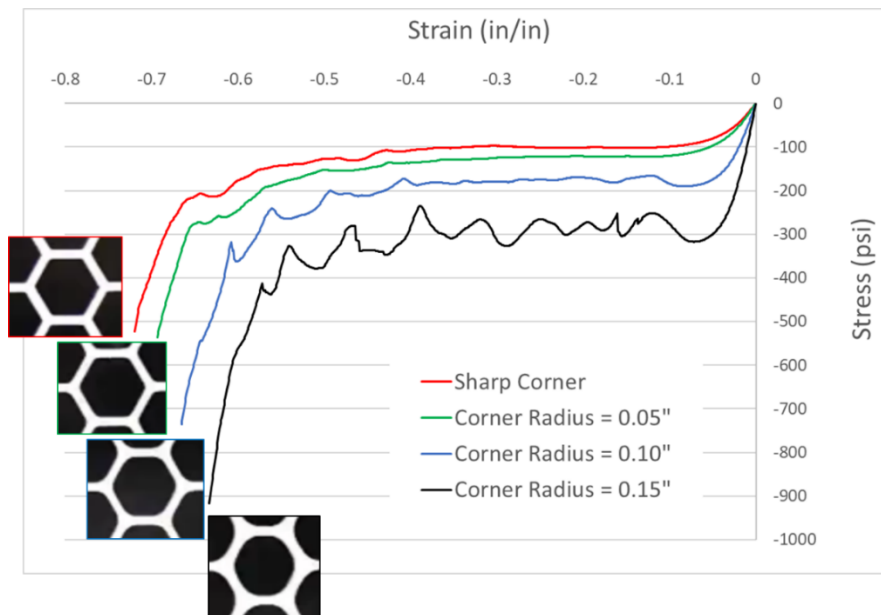
When investigating biological samples and how different aspects of their structure affect performance, mechanical testing cannot always be performed on the samples. Most mechanical testing is destructive in nature and while our samples could not be altered in anyway, there are more reasons for not testing each sample that was found. No two nests are quite the same, conducting mechanical tests on two nests even from the same species will give different results. Any conclusions that could be made from testing these biological samples would not be statistically sound. Identifying how varying different aspects of the structure influence the overall performance cannot be measure either because the biological samples have their own ranges of relations. This section will discuss what features were chosen to replicate and a design of experiment that was conducted to investigate how varying these features affect overall performance.

#### 3.1 Two-Dimensional Design

The data generated in the study of insect nests was used as part of a NASA-funded project with a local small business. As part of this, mechanical testing was conducted on SLS specimens, see Figure 29 (a) and (b) to assess the effect of corner radius on the behavior of the structure. As shown in Figure 29 (b), there is a gradual increase in in-plane compressive stiffness and first maximum stress, and while the plateau generally rises, strain at densification strain reduces. The identical test scenario was evaluated using ANSYS, validating that the highest specific stiffness and lowest specific maximum stress in a honeycomb occur when the corner radius approaches the cell radius (full circle) and the thickness of the walls is at its highest in relation to the cell diameter (Figure 30)



(a)



(b)

Figure 29: (a) SLS honeycombs with varying corner radii under compression, (b) Effective stress-strain curves for the four different radii studied (Courtesy Bharath Santhanam)

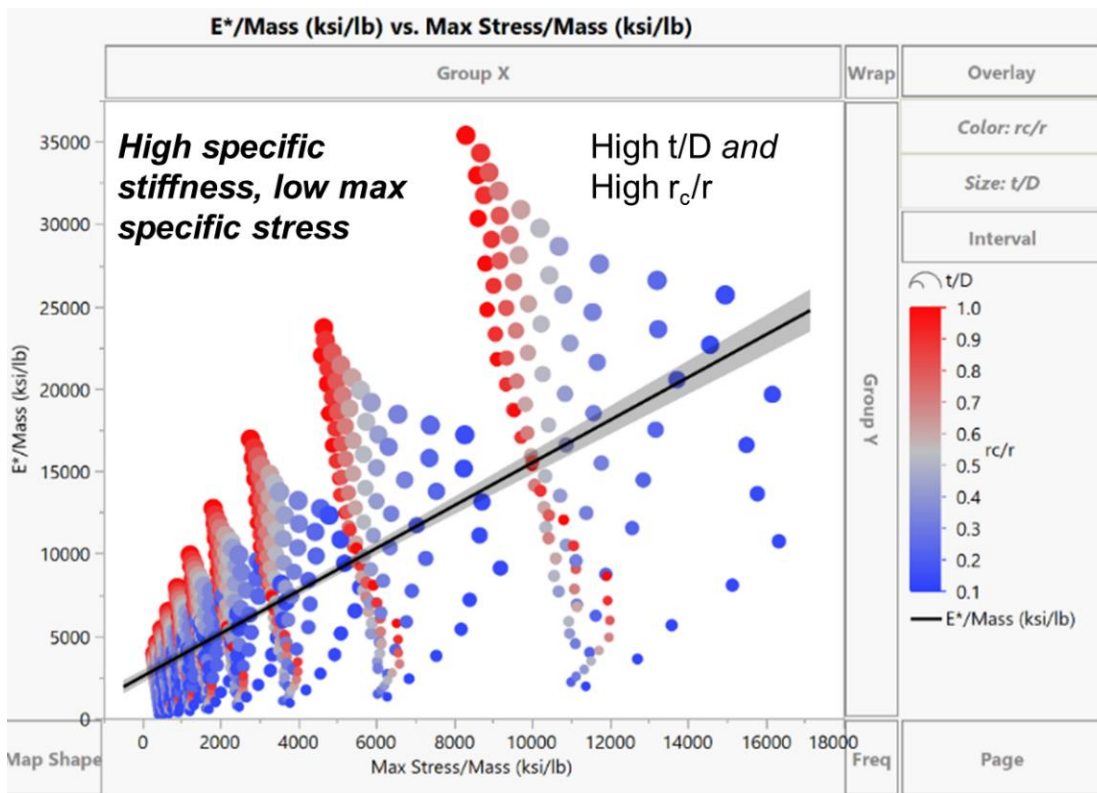


Figure 30: Results from an ANSYS parametric optimization (Courtesy Alex Grishin, PADT Inc.)

The focus of this thesis work was however, on studying design parameters out-of-plane, and it is to these that we now turn.

### 3.2 Three-Dimensional Design

The last chapter primarily focused on an idealized two-dimensional structure located at the top of the insect nests. This section will be discussing the third dimension of bee honeycomb and how cells terminate throughout the structure. Wasp nest cells terminate in a much less uniform and periodic manner, so they are excluded from study at the moment. Current honeycomb sandwich panel core is a two-dimensional lattice extruded into the third dimension. In observing natural

honeycomb, it can be seen that these structures are not quite as simple. The specific function of the design elements that will be discussed is not known but this work attempts to explain so benefit to these designs.

### 3.2.1 Cell Opening Coping

The first step in studying these three-dimensional structures is understanding the limitations in the previous two-dimensional work. In the previously mentioned work, the opening of cells was scanned, and the corner radius, wall thickness, and cell diameter were measured. By looking at a cross section of a Micro CT scan, Figure 31, it can be seen that what was idealized as the wall thickness is actually a measure of what is called coping. This coping is a buildup of wax at the opening of each cell within a natural honeycomb. With this distinction between coping and wall thickness the question arises: what does this extra material lend to mechanical performance? Later in this study, a design of experiments is created with coping as one of its factors.

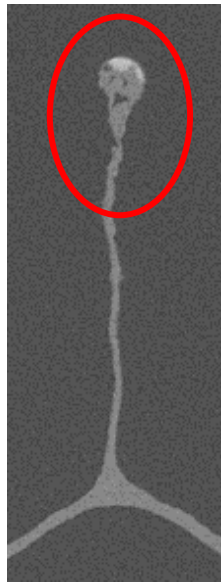


Figure 31: Cell coping

Within this work, a secondary study was conducted to look more closely at the true wall thickness at various points. From the previously mentioned Micro CT scan data, one cell wall, see Figure 32, was examined. To reduce processing requirements and computation speed, this wall was cropped out of the overall scan data. The CT scan data is made of hundreds of stacks of two-dimensional images which can be used to represent the full three-dimensional object. A CT data analyzing software called Aviso is used to manipulate scan data into stacks of the desired location within the object. For the cell wall in question a stack of four hundred and fifty images is cropped out from the one thousand one hundred available. Each stack is thirteen point five eight micron thick. In Aviso, a script was made to measure the max dimension in the "X" direction at each slice.

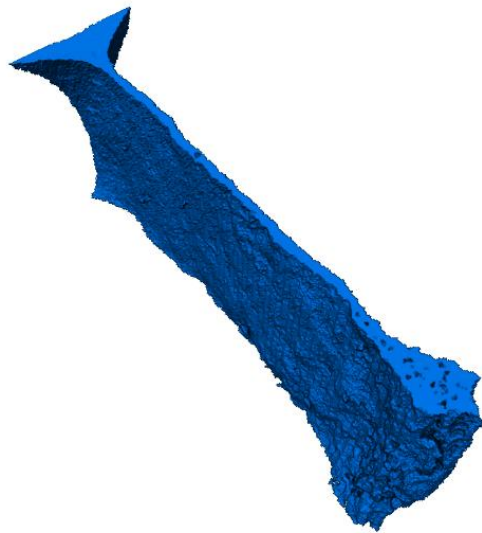


Figure 32: Cell wall used for thickness study

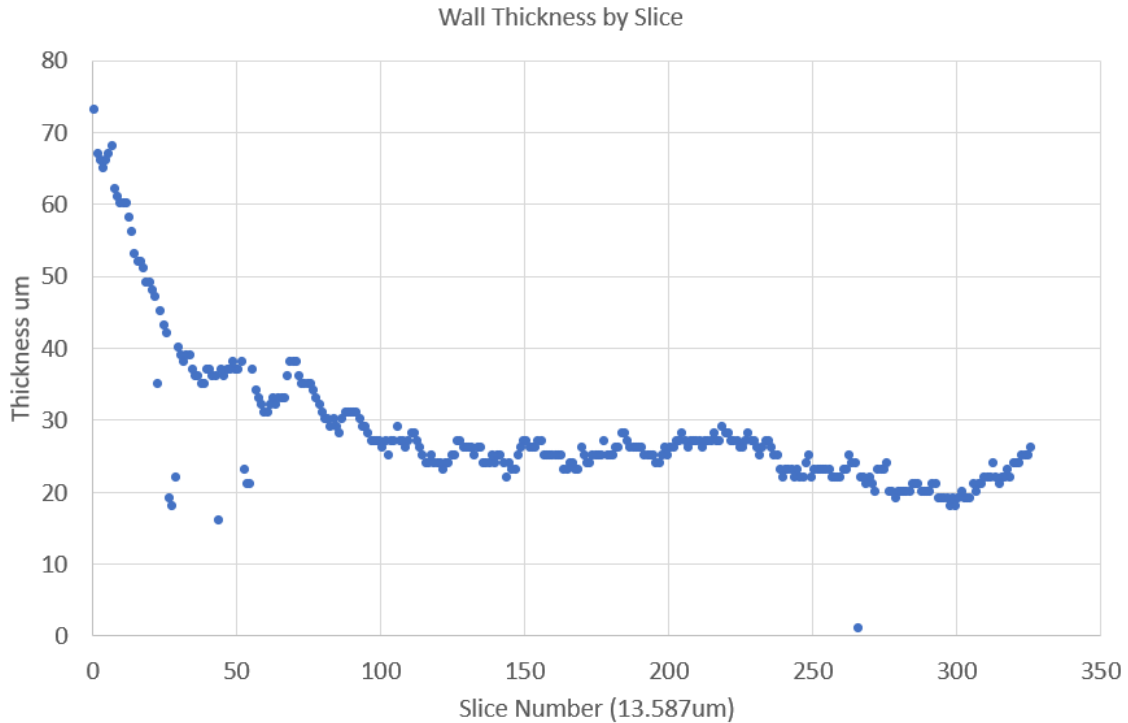


Figure 33: Wall Thickness by Slice Number

Figure 33 shows how the wall thickness of the selected wall varies from the cell interface, the left of the graph, to the cell opening, the right of the graph. The chosen stack used for these measurements included some of the interface and cell opening, which can be seen as the sharp increases at either end of the data above. It can be observed that the dimensions in between the above-mentioned cell features is relatively flat at the different locations within the wall. As this is just one cell wall from an entire comb, future work would include conducting a similar analysis across multiple cell walls through out a given sample.

### 3.2.2 Cell Wall Interface

Another feature of natural honeycomb that is apparent in the third dimension without having to Micro CT scan a sample is the interface between the two walls of cells in a comb, see Figure 34. This interface terminates each of the cells and runs



along the center of a comb from the base all the way to the edge where the comb is being added to and altered. In Figure 35 it can be noted that each wall of cells does not match up perfectly with the opposing wall. Rather, they are skewed from one another in such a way that the vertex of three cells on one side falls in the center of a single cell on the other. This is not an isolated occurrence; this can be seen throughout the entire comb. This alignment of cells leads to a geometry that is more difficult to visualize without the help of Micro CT, see Figure 36.



Figure 34: Walls of cells and interface



Figure 35: Opposing walls of cells

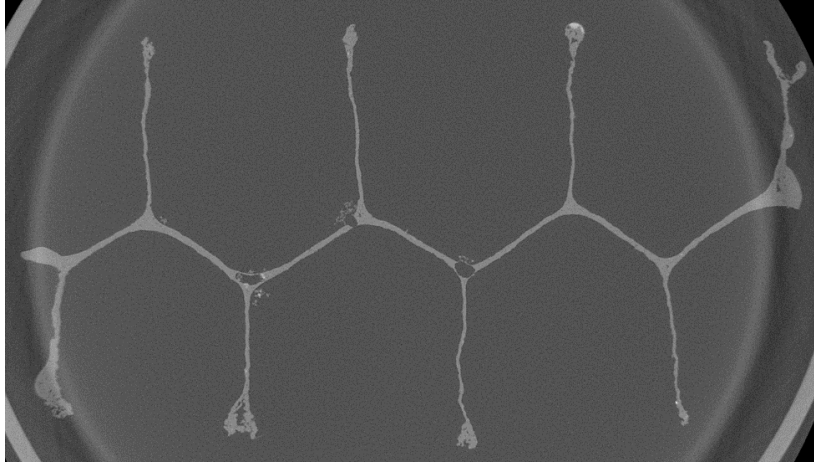


Figure 36: Micro CT of cell interface

However, at the time of investigation of this interface, Micro CT was not available to shed light on the internal geometry. Initially, this geometry was replicated in CAD in order to understand the three-dimensional aspect of the cell interface. A literature review was later conducted on this interface to confirm the initial findings, but this initial effort was not put to waste and used as the archetype for the CAD models used in manufacturing to come later in this study. While replicating the interface in CAD, assumptions that were first made about the geometry proved to be un-true. The main assumption accepted were the hexagonal cell walls all terminated at the same location and then the interface was formed. As can be seen in Figure 37, each cell wall terminates along a line defined by the interface itself. With this discovery, the rhombi discussed in the Section 2.2 can now be created properly. This shape, three rhombi leading into a hexagon is a truncated rhombic dodecahedron. This shape used in natural honeycomb was studied in 1965 by László Fejes Tóth, who concluded that this was not the optimal geometry to nest these cells. However, the true optimal geometry was so similar, less than a tenth of a percent more efficient than what occurs in nature is considered the optimal method.

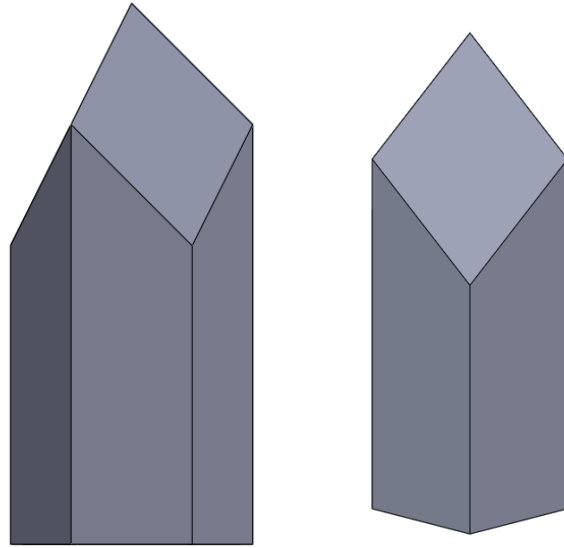


Figure 37: Cell wall termination

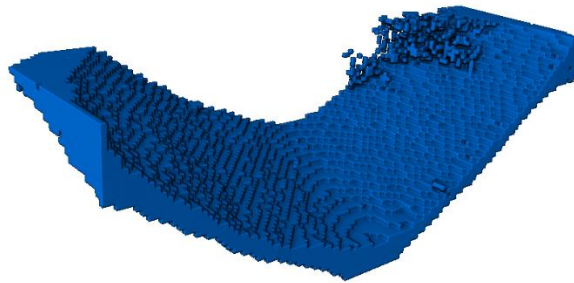


Figure 38: Cell interface sample used for angle study

Using the same CT scan data from the wall thickness study, the cell interface angle was also investigated. As with the wall thickness measurement, a stack is cropped from the entirety to reduce computation time. Within Aviso, no tools were available to measure the angle of features within a three-dimensional object. To measure this angle, two lines were created on the stack; one representing the center

of the cell, and the other represents the interface surface. From these lines, an angle of fifty-seven point zero two was observed. With only one cell interface measured, more instances of the cell interface should be investigated for a more statistically sound conclusion of this dimension.

### 3.3 Design of Specimens

Investigating the mechanical properties of the before mentioned parameters required the design and manufacturing of specimens that could undergo testing and be replicated with ease. Selective Laser Sintering (SLS) was chosen as the manufacturing process because of its design flexibility and the convenience of having the specimens made on the Polytechnic campus [14]. As will be discussed in greater detail later, many of the specimen designed have multiple over hangs and internal geometries too complicated to be manufactured through traditional manufacturing processes. As SLS is a powder-based printing technology, parts with overhangs can be created without supports needed which reduces post processing time and allows faster iterations of parts to be made. Before the complex internal geometry was designed, the overall size of each specimen was determined. According to MILSTD-401, specimen size for cells one half inch and smaller is 76.2mm x 76.2mm x 12.5mm for compression testing and 203.3mm x 76.2 x 12.5mm for bend testing. With these overall dimensions defined, cell diameter and wall thickness were next defined as eight millimeters and one millimeter respectively. These parameters where chosen together in order to achieve a cell density of ten by ten within the smaller compression samples.

### 3.3.1 CAD Modeling of Specimen

As stated in section 3.1.2, a CAD models of the internal interface had already been created by the time the study was ready to create test specimen. However, the models did not fit the dimensions mentioned previously and they lacked other parameters of interest. While the models themselves could not be used, the insight gained from them was used to create robust new models that could be modified at will in order to create new variations. One key aspect of the study was the ability to vary the previously defined parameters, this means the CAD models had to accommodate this requirement. For ease of modeling, the Design Table functionality in Solidworks was utilized to create variations of a CAD model within a single file. Eight archetypal models had to be made in order vary all of the parameters of interest without creating errors within the CAD software. As will be explained in the next section in greater detail, some parameters are removed from specific variations within the DOE. Within the Design Table, parameters can be given multiple dimensions and Solidworks will re-solve the model depending on which dimension is chosen. In the case of a parameter that is remove, Solidworks will not allow for a dimension to not exist within the Deign Table. Each of the archetype models is missing a parameter, allowing those specific combinations from the DOE to be created. See Table 3 for a more detailed description of the CAD modeling and Figure 39 for a diagram of varied parameters within a single cell.

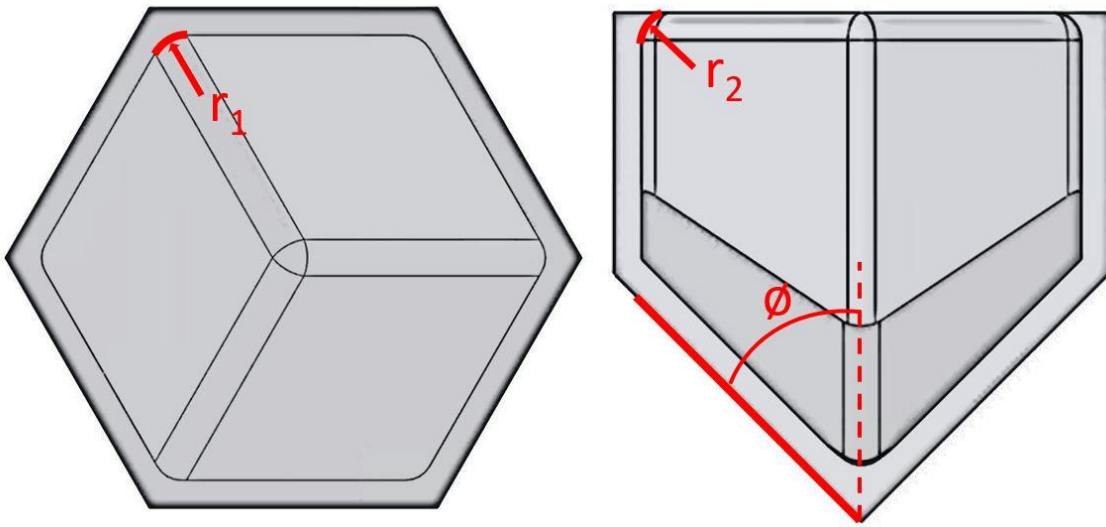
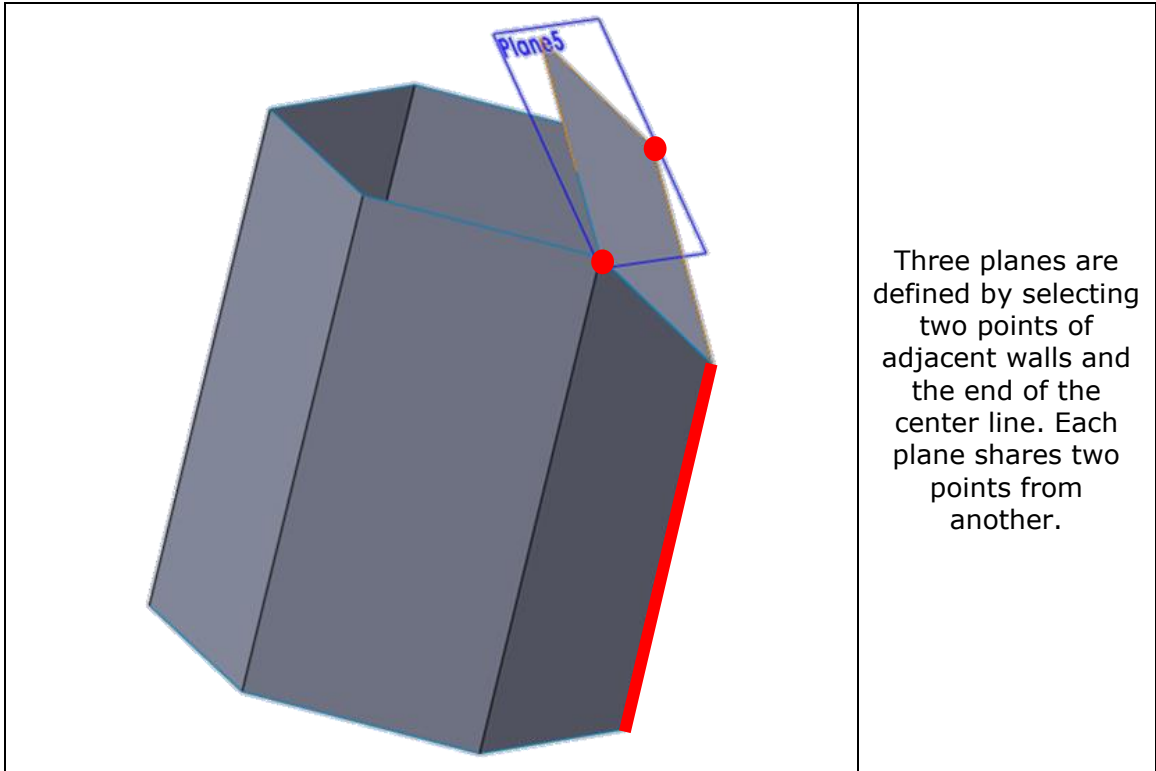
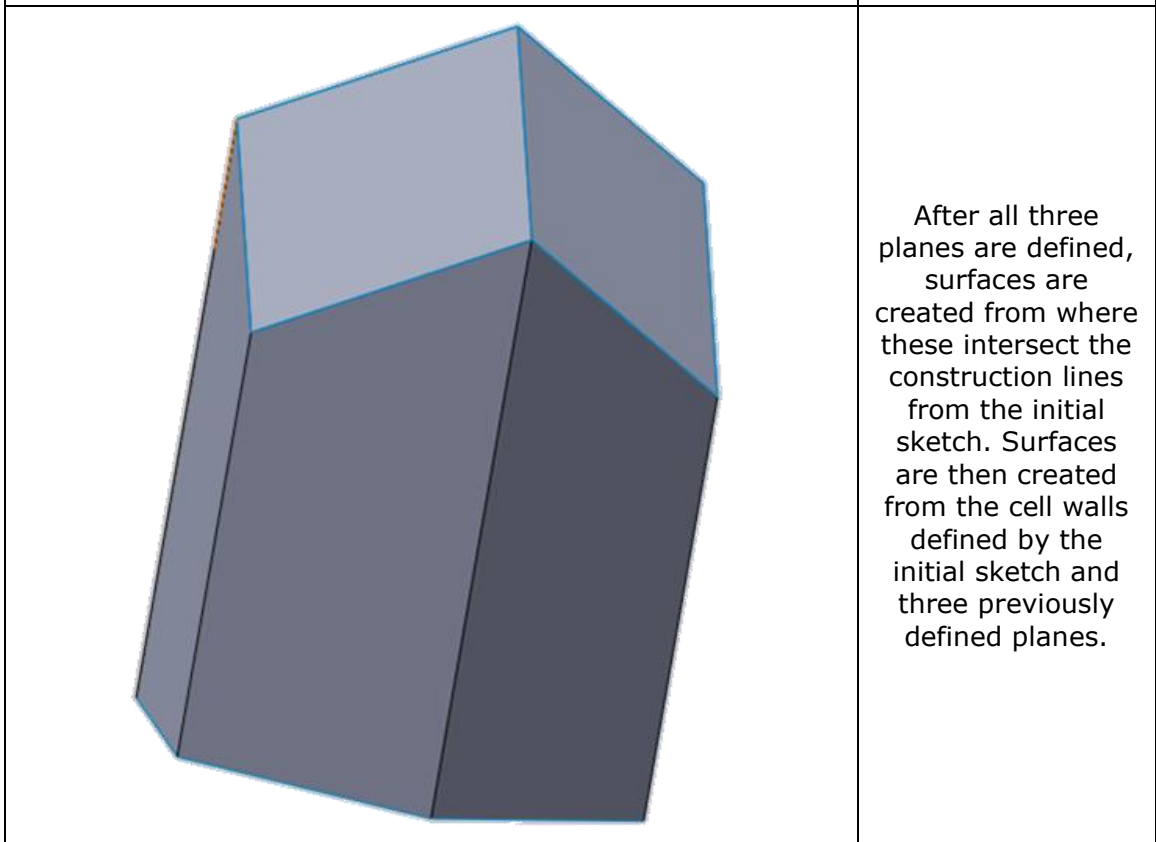


Figure 39: Cross section of single cell

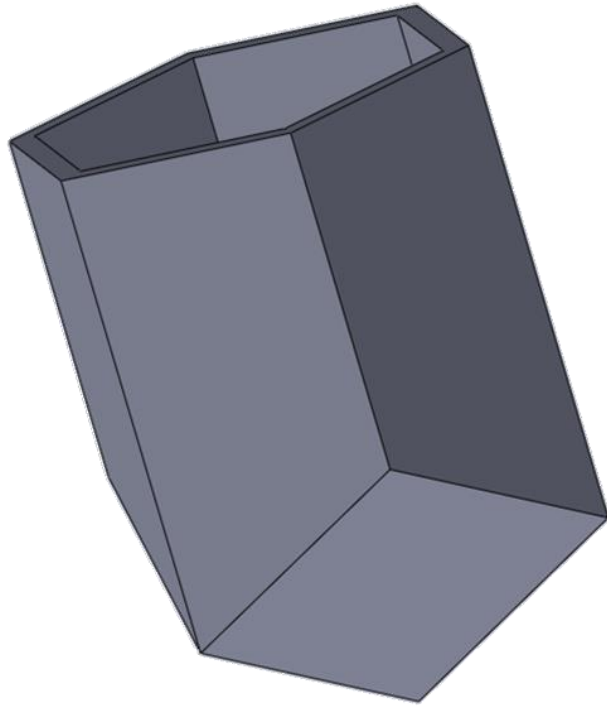
<p style="color: red; font-size: 2em; margin-left: 10px;">*</p>	<p>A hexagon with an inscribed circle defining the cell diameter is used as reference for construction lines. The depth of the cell interface is defined by the angle between the edge of the hexagon to the end of the center line.</p>
---	--



Three planes are defined by selecting two points of adjacent walls and the end of the center line. Each plane shares two points from another.

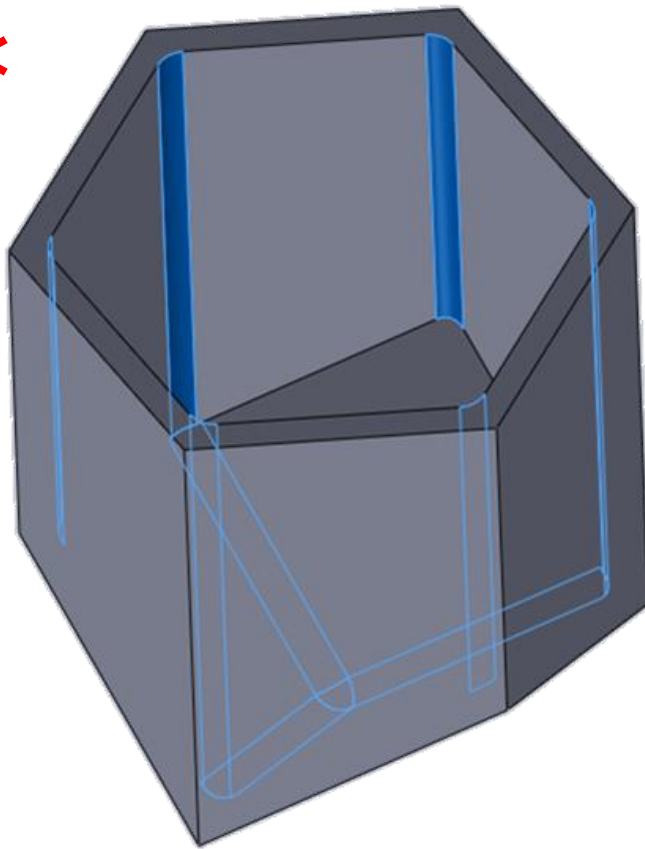


After all three planes are defined, surfaces are created from where these intersect the construction lines from the initial sketch. Surfaces are then created from the cell walls defined by the initial sketch and three previously defined planes.



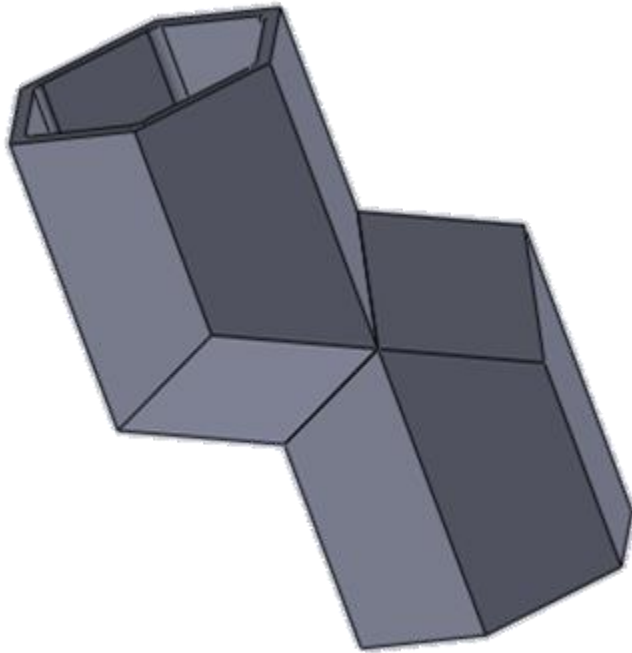
With all nine surfaces created, they are stitched together and thickened as an entity. This entity is given a thickness of half a millimeter.

This is done because once two cells are mated together, the cell wall doubles and becomes the desired thickness of one millimeter.

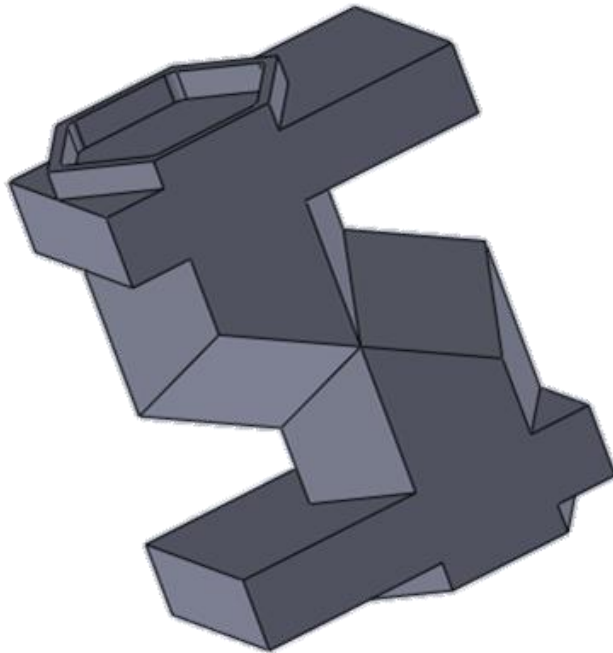


Now that there is solid body that can be manipulated, the internal corner radius is added to all the vertexes on the body.

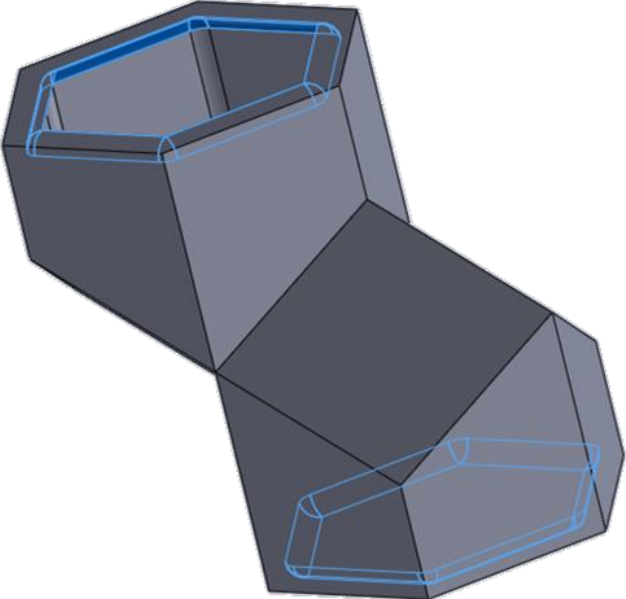
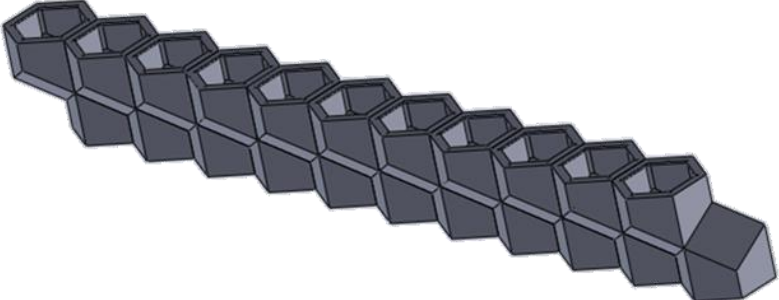
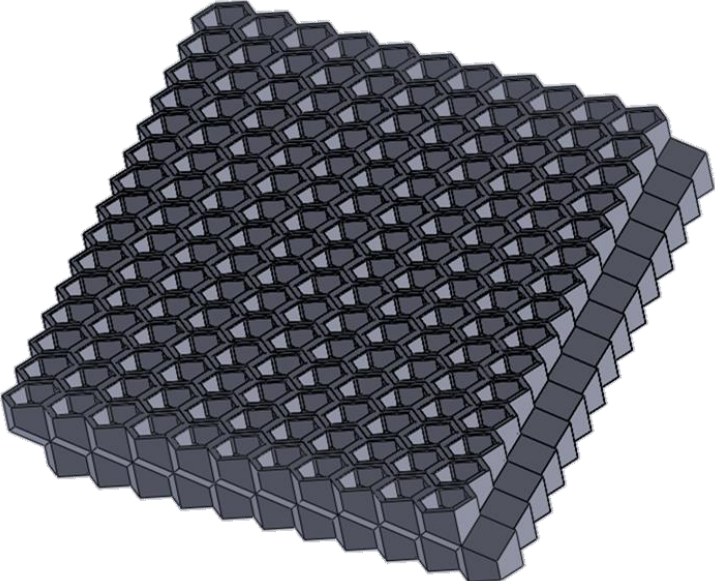




The cell is then duplicated and rotated so one rhombi from each cell can be mated together.



Rectangular bodies are added to each cell to both define a plane for the coping to be added to and the total height of the specimen.

	<p>These rectangles and the excess height of the cells is cut away revealing the coping and cell opening.</p>
	<p>With two fully defined cells on either side, a linear sketch pattern is made to create a row of cells.</p>
	<p>Another linear sketch pattern is created from the previous, to form a full array of cells.</p>

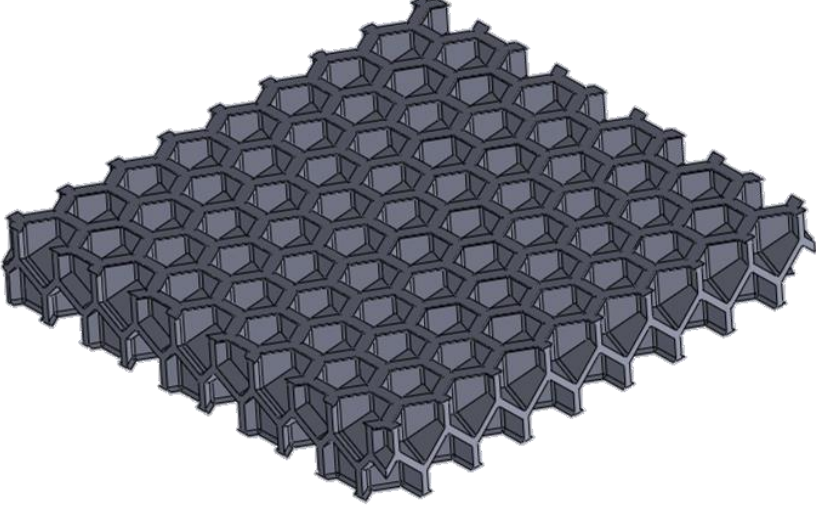
	<p>Finally, the overall dimension defined previously, different for compression and bending samples, are cut out from the mass of cell revealing the final model.</p>
<p>* Steps that feed into Design Table</p>	

Table 3: Specimen modeling steps

### 3.3.2 Design of Experiment

The geometric features discussed previous sections are both interesting in their own right but this study is interested in how they affect mechanical behavior for the entire structure. Not only do they have the potential to affect specific aspects of mechanical behavior, how these aspects are affected by the combination and variation of these features is also a point of interest. To test how these features, affect mechanical behavior, specimens were manufactured, tested, and compared to one another. Before the entirety of the compression CAD models were created, a Design of Experiment or DOE was conducted to determine what variations of these parameters would be investigated. The parameters varied were the angle that defines the depth of the cell interface, the radius of coping and the internal radius of each cell. Internal radius was included in this study because it can be observed in all insect nests regardless of material or species. See Table 4 for a table of DOE combinations.

A full factor DOE was chosen in order to fully explore how each chosen parameter worked together to impact mechanical performance. At three factors and four levels, this DOE contains sixty-four different combinations of parameters. Within the DOE, each parameter was chosen deliberately to study a range of variability within the given space. Interface angles fifteen degrees apart from each other were chosen in order to determine where within a ninety-degree span, mechanical properties were optimized. Radii, both internal and for the coping, of one half, one and two millimeters were chosen to how different scales affected mechanical properties. As two is double one which is double one half, these radii spanned a range of what could fit within the given cell size. A value of zero within the DOE represents the omission of this parameter. This research also hoped to gain insight into if the defined parameters were needed at all.

<b>Parameter</b>	<b>Removed</b>	<b>Min</b>	<b>Mid</b>	<b>Max</b>
<b>Interface Angle</b> (Degrees)	0	30	45	60
<b>Coping Radius</b> (Millimeters)	0	0.5	1	2
<b>Internal Radius</b> (Millimeters)	0	0.5	1	2

Table 4: Full factorial DOE

The above DOE describes parameters and their variations for the compression samples within this study. Originally, it was planned that the bending samples would be manufactured using the same DOE for its variations. With the deadline of the study fast approaching, it was decided to create a smaller testing sample for being samples. The parameter of most interest with regard to bending was the interface between cell walls. The same variations of no interface, thirty, forty-five, and sixty degrees were chosen for bending samples, the only difference is three copies of each variation are printed as well.

## CHAPTER 4

### ADDITIVE MANUFACTURING OF HONEYCOMB CORE

This section begins by giving a description of the manufacturing process chosen to create specimens for mechanical testing. A process flow from CAD model to parts in hand is laid out with key steps notes and explained. Everything explained in this section applies to both compression and bending specimen.

#### 4.1 Selective Laser Sintering (Nylon 12)

Additive manufacturing processes have the advantage of allowing complex geometries and features to be created without extra manufacturing effort from an engineer or technician. Adding extra features such as fillets or chamfers to a traditionally machined part requires extra tool changes and extra time to make the necessary tool paths. Because additive manufacturing is an iterative rather than a subtractive process, that is material is deposited layer by layer, these extra features only change tool paths which can affect the overall time of manufacturing but by fractions of a percent. With powder-based systems using a laser to melt powder to form parts, no tool changes are required at any point in the printing process. With this flexibility in design and material allocation, parts can be made with additive manufacturing that cannot be made with any other manufacturing technique. Internal features for example, see Figure 40, cannot be created from one block of material even with the most sophisticated CNC machine. When trying to replicate biological specimens and designs, not being limiting by geometry allows for researchers to more accurately study their properties. A EOS Selective Laser Sintering printer located in TECH 199 on the Polytechnic campus was used for manufacturing specimen.

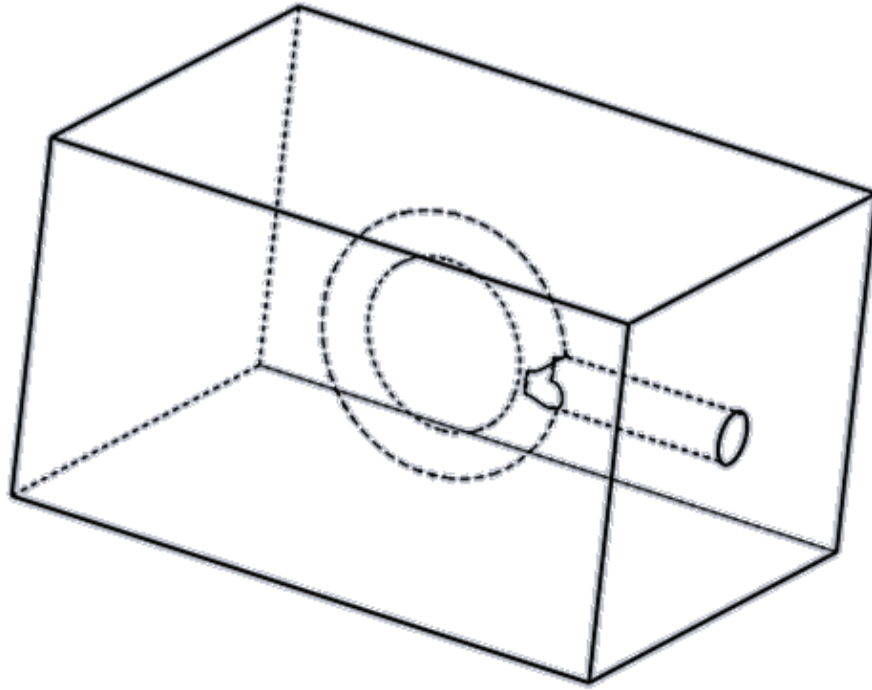


Figure 40: Complex internal geometry example

Selective Laser Sintering or SLS, see Figure 36, is a powder based additive manufacturing technology that is primarily used for rugged, end use parts and prototyping of complex designs. Unlike most additive manufacturing technologies, SLS does not require parts to be supported or attached to the bottom of the build area. This provides more advantages for this study; the over hangs that exist in a majority of the design models can be printed without supports needing to be removed from each cell once the parts have completed printing. Before printing, the CAD models discussed in the last chapter are converted to a stereolithography or STL file. By converting to this file type, features and dimensions assigned within a CAD software are translated to a mesh of triangles. This mesh is imported into a software designed to manipulate and repair STL files. Once in this software, Materialized Magics was used for this study, all sixty-two STL files are imported into a project file that contains constraints from the printer. These constraints give the dimensions of

the build volume and where within the volume parts can be placed. Magics has built-in tool that can be used to auto nest parts within this build volume to minimize the amount of powder used for a print. Within this tool, spacing between parts is defined as five millimeters and spacing between parts and the sides of the build volume is defined at ten millimeters.

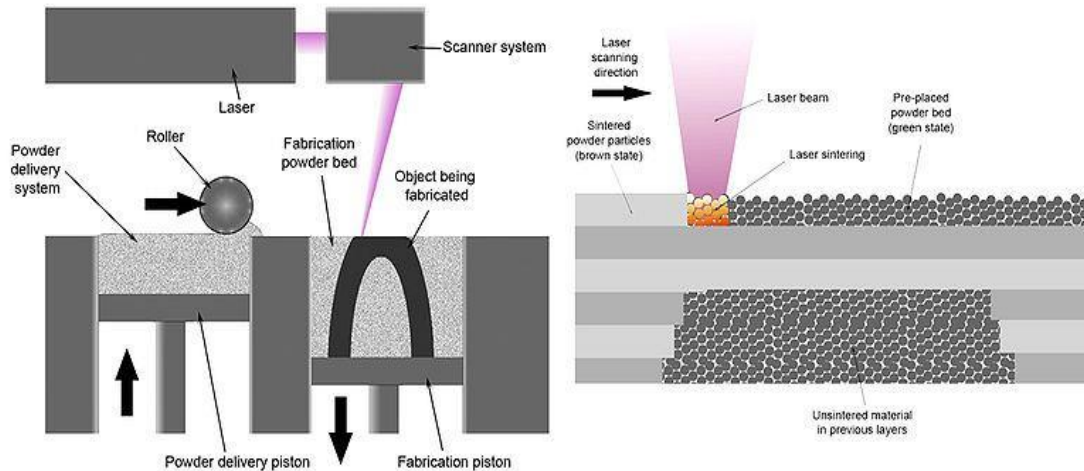


Figure 41: SLS printing process [14]

With the orientation and location of each STL file in the build volume created, slices are taken at each defined layer height and converted to toolpaths. Toolpaths are loaded into and used by the printer to guide the laser into the correct positions to create the previously defined CAD models. Once the print is started with the EOS, the build volume is heated internally to raise the temperature of the Nylon powder to just below its melting point. A ten-millimeter layer of powder is deposited to the build volume for parts to start being sintered. As each slice is sintered, a new layer of powder is rolled onto the last repeatedly until the last required layer has been deposited. After the completion of the printed parts, the build volume is allowed to cool back to room temperature.

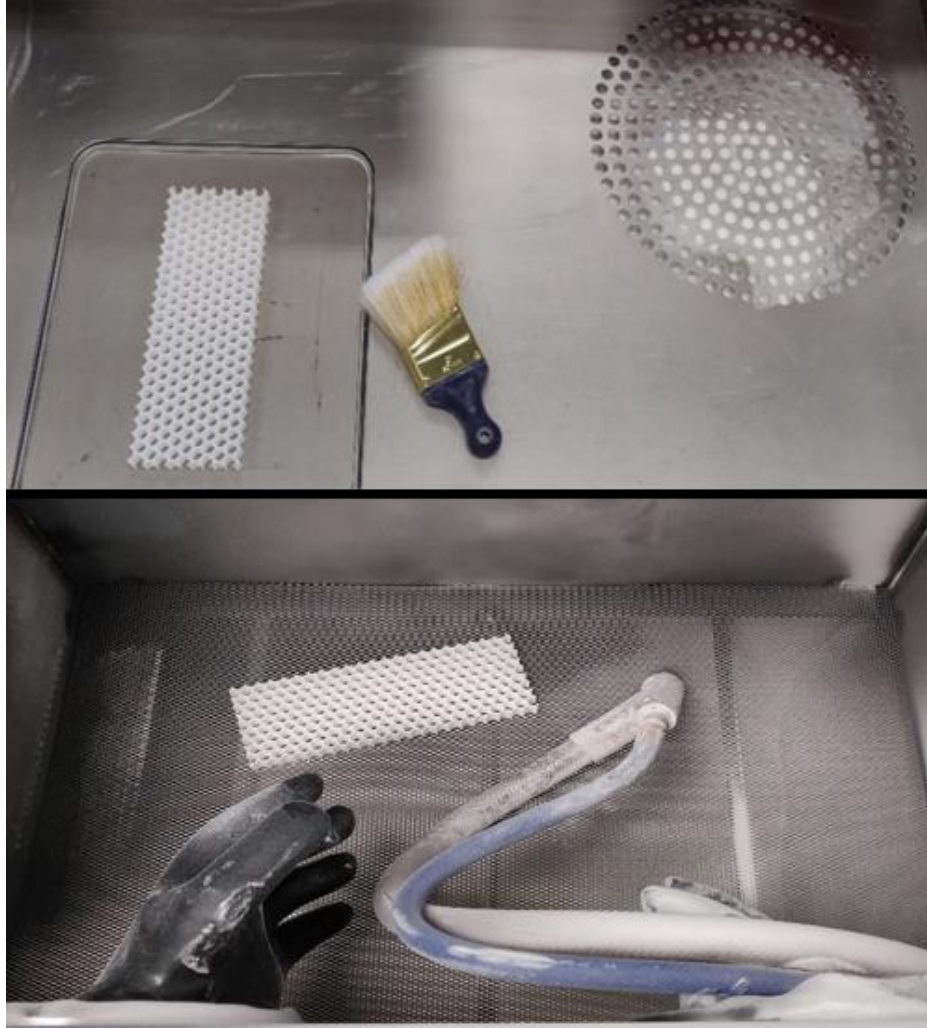


Figure 42: SLS powder removal steps

Post processing is a necessary step for any manufacturing process and even though SLS does not require the removal of supports, excess powder must still be removed from any hole or internal geometry. Initially, each part is removed from the build tank and brushed off to remove powder clinging to the surface. During this step, each sample is also labeled with a unique serial number to identify it before and after mechanical testing. To remove trapped powder within each cell, samples are placed inside of a glove box and blown off with compressed air. A glove box is utilized to contain the left-over powder. Each sample is inspected, and hand tools are



used to remove powder from specific location in the specimen. Samples are then rinsed with water and blown off one last time to ensure all excess powder has been removed. See Figure 42 for an example of powder removal steps. See Figure 43 for examples of samples post processing.

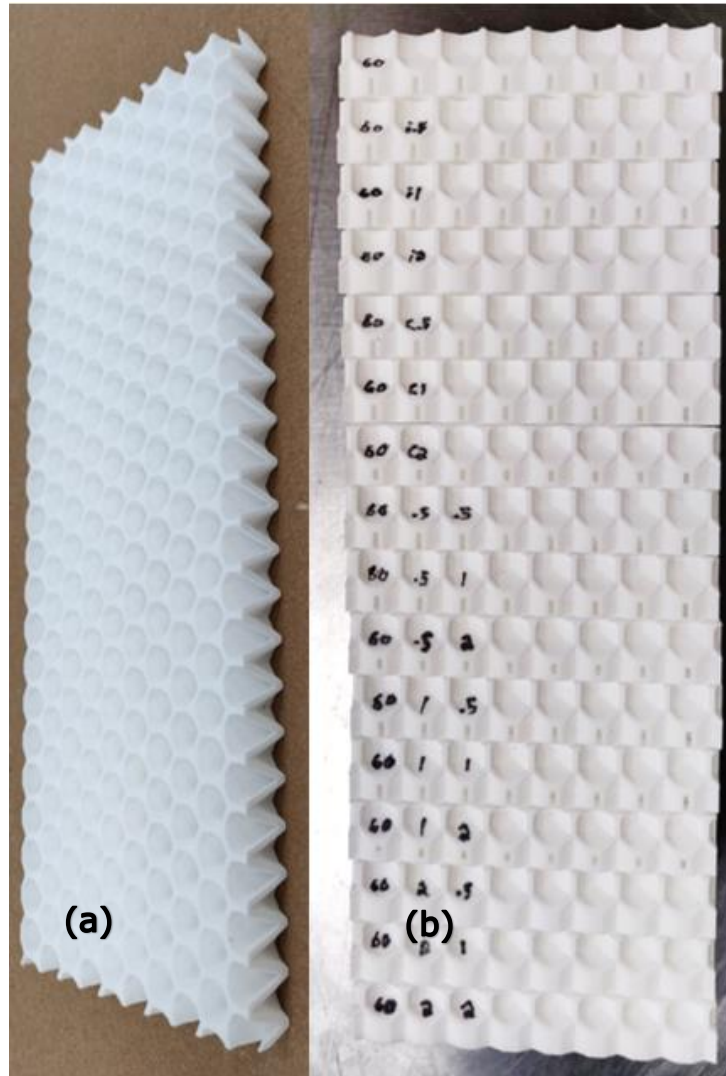


Figure 43: (a) Bending and (b) Compression samples

## CHAPTER 5

### MECHANICAL BEHAVIOR

This section describes aspects of mechanical testing conducted for this study including test fixturing, test methods, and test results. Specifics of each type of test conducted, compression and three-point bending, are taken from multiple testing standards found during literature reviews. Strain rates used for compression testing were taken from MIL-STD-401. All specimen dimensions and fixture specifications were taken from MIL-STD-401. ASTM D790 was referenced for strain rates for three-point bend testing as well as equations for calculating flexural properties. Compression testing is conducted in order to calculate elastic modulus, first maximum stress, and energy absorption. Three-point testing is conducted to calculate maximum load and flexural rigidity.

#### 5.1 Testing Setups

An Instron 5985, see Figure 44, was used for all mechanical testing for this study. This Instron has a 250 kN load cell which is overkill for many applications. However, an Instron with a 50 kN load cell was initially used for testing compression samples and the first three samples maxed out the load cell within the first millimeter of travel. The choice was then made to transition all testing to the higher load capacity system in order to capture more of the force displacement curve for each of the compression samples. Despite the load capacity, the Instron 5985 was chosen to conduct the three-point testing as this equipment already had a three-point bend fixture available. Bluehill Universal software used to control the Instron was utilized to create each of the test methods for this study. Within this software, the user can specify what triggers and ends a test. Calculations can be made during the test procedure and at the end of each test,

user chosen data is exported a CVS file to be used for data analysis. While the Bluehill Software can be used to calculate stress, strain, flexural rigidity, and more, it was chosen to take the raw data from these tests and calculate the desired attributes with statistical analysis tools.



Figure 44: Instron 5985 250kN Load Frame

#### 5.1.1 Quasi Static Compression

As for the physical set up of the compression testing, compression platens, see Figure 45, with a spherical seat are installed onto the Instron. The spherical seat is loosened to rotate freely, the crosshead is then lowered until the platens are contacting on another. A load of forty-five newtons is applied to the load head to ensure the plates have made complete contact with one another. Now that the platens are parallel, the spherical seat is tightened into place. Next, each sample is

centered within the compression platens; without samples being centered, damage can occur to the test frame from the platens rotating as the test commences. To center the samples, a marker is used to indicate where two adjacent sides of a sample need to lay on the platens. With the samples centered, the crosshead is moved down until the top compression platen contacts the sample. To avoid applying a pre-load to samples, the crosshead is raised at small increments until no load is detected from the loadcell. At this point, the load frame origin is set to zero and from this point, our test will travel nine and a half millimeters.



Figure 45: Compression platens with sample

A strain rate of  $2.5 \times 10^{-3}$  mm/mm/min was used for the quasi static compression testing in this study. MIL-STD-401 prescribes a strain rate in which testing will complete within three to six minutes. With an overall thickness of twelve and a half millimeters and a total displacement of nine and a half millimeters, this strain rate gives tests that complete in slightly longer than five minutes. At the conclusion of each test, a CSV file is exported and saved to be used for data analysis.

### 5.1.2 Three Point Bending

Much like the compression testing, a new fixture is required for three-point bend testing. Unlike the compression fixture, no load is applied during installation. With the loading nose is attached to the load cell and the support is attached to the jaws below. Next, the adjustable supports are loosened to move freely in the horizontal direction. The crosshead is lowered until the loading nose is below the top edge of the supports. Each support is moved until it comes into contact with the loading nose and external pressure is applied by hand to ensure the mating surfaces are parallel. With both halves of the fixture parallel, each can be locked into place, see Figure 46. Supports are then moved to 152.4 millimeters from one another per MIL-STD-401. Once samples are placed on the test fixture, the cross head is moved down until the load nose makes contact. The crosshead is then raised in small increments until the load cell displays no load. At this point, the crosshead origin is set, and testing can commence. A strain rate of 0.1 mm/mm/min was used for the three-point bend tests per ASTM D790. This standard also calls for testing to end when five percent strain is reached. For these samples of twelve and a half millimeters, this would be a displacement of only 0.625. A displacement of 1.25 millimeters, which equates to a strain of ten percent, was used to ensure enough data could be gathered from each sample in order to conduct data analysis.

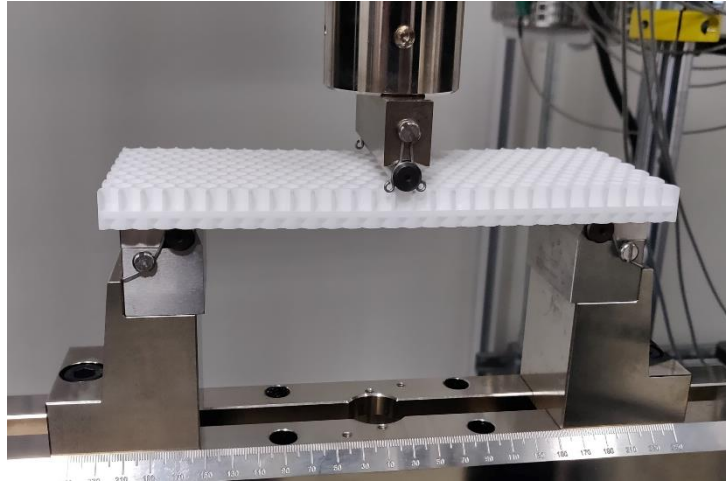


Figure 46: Three-point bend fixture with sample

## 5.2 Data Analysis

Microsoft Excel, MATLAB, and JMP 14 were used for data analysis of the raw mechanical testing data. Manipulations of raw data and mechanical property calculations were done using both Excel and MATLAB. JMP was used to plot mechanical properties of samples against one another to draw statistical conclusions and test for statistical similarities.

### 5.2.1 Quasi Static Compression

The following figures contain raw load vs displacement data straight from the Instron 5985 for the compression tests. Each of the four plots is split up by the interface angle defining the set of samples. This raw data formed the basis for calculating the effective material properties, modulus of elasticity, first maximum stress, and energy absorption. First, raw load displacement curves data are converted to stress strain curves by dividing force by the cross-sectional area of the samples and by dividing displacement by the overall thickness of the samples. Cross-sectional area is five thousand eight hundred and six millimeters while specimen thickness is twelve and a half millimeters. Now that this data has been converted to

stress and strain, the mechanical properties mentioned above can be calculated. Modulus of elasticity is defined as the slope of the elastic region of the stress strain curve, see Figure x(a). Most moduli can be calculated from 0.05 and 0.15 strain; however, some samples required this range to shift in order to use data only within the elastic regime. A value for first maximum stress is taken from the curve right before the samples starts to yield for the first time, see figure x(b). As with moduli, the range in which this value is found sometimes needs to be manipulated given different sets of data. Finally, energy absorption is calculated as the area under the stress strain curve, see Figure 47(c). For this calculation, the trapezoidal method is utilized to best approximate the area under the curve. Boundaries for each trapezoid are defined by each time step given from the raw load displacement data for the most accurate result.

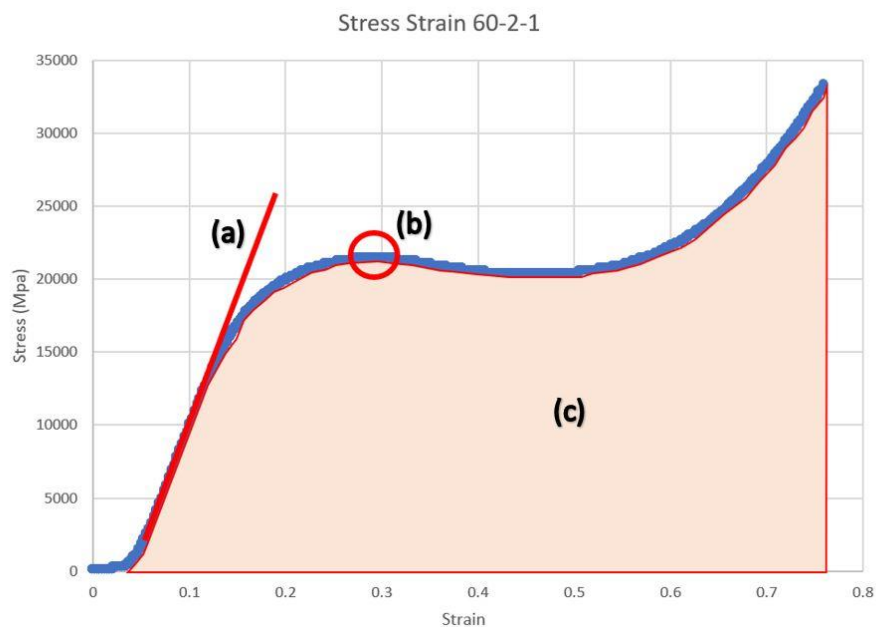


Figure 47: Compression calculations on stress strain curve (a) Modulus of Elasticity  
(b) First Maximum Stress (c) Energy Absorption

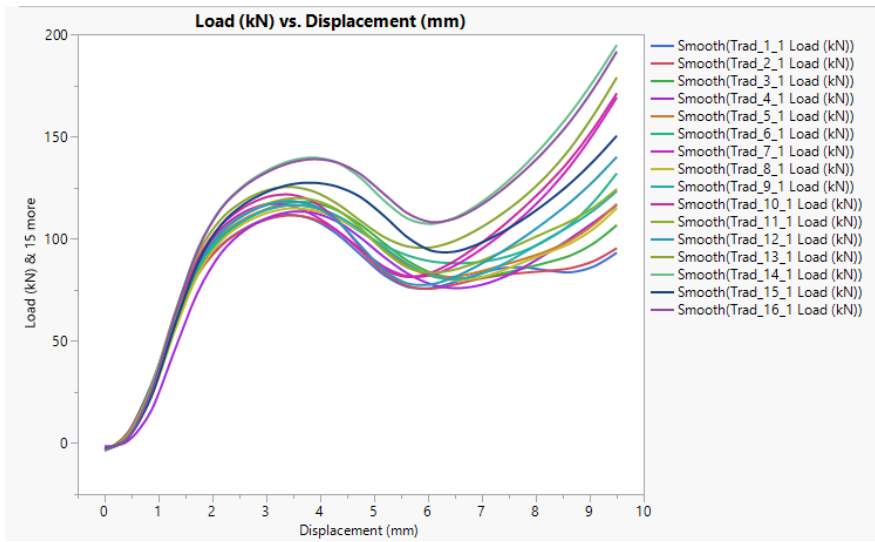


Figure 48: Load vs displacement data for traditional samples

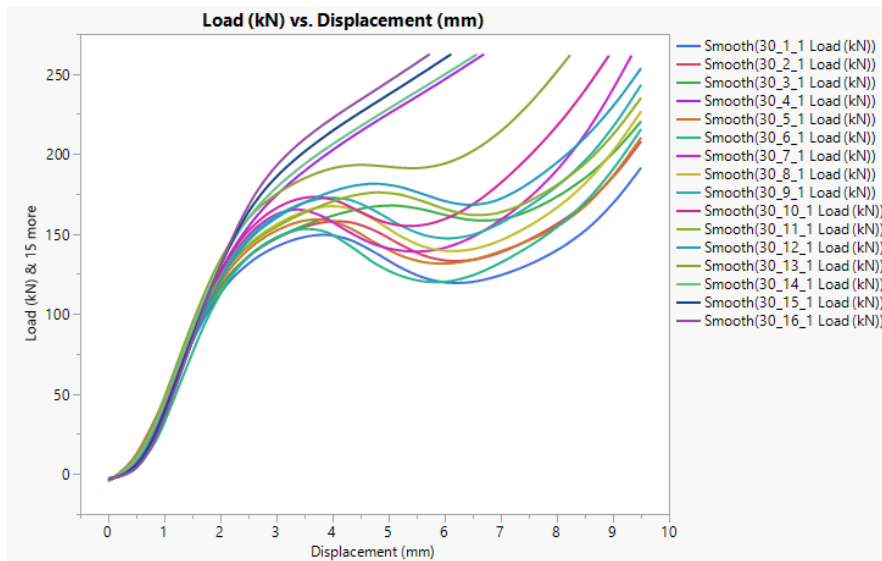


Figure 49: Load vs displacement data for 30-degree samples



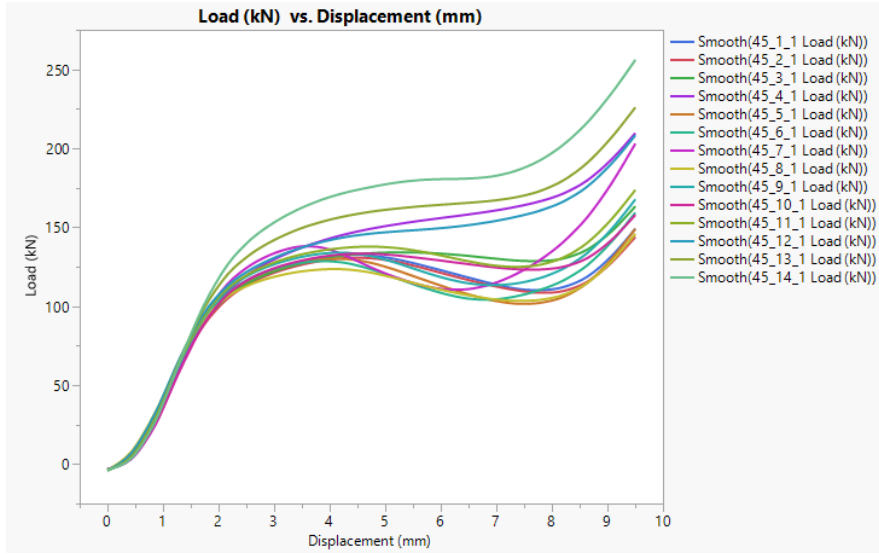


Figure 50: Load vs displacement data for 45-degree samples

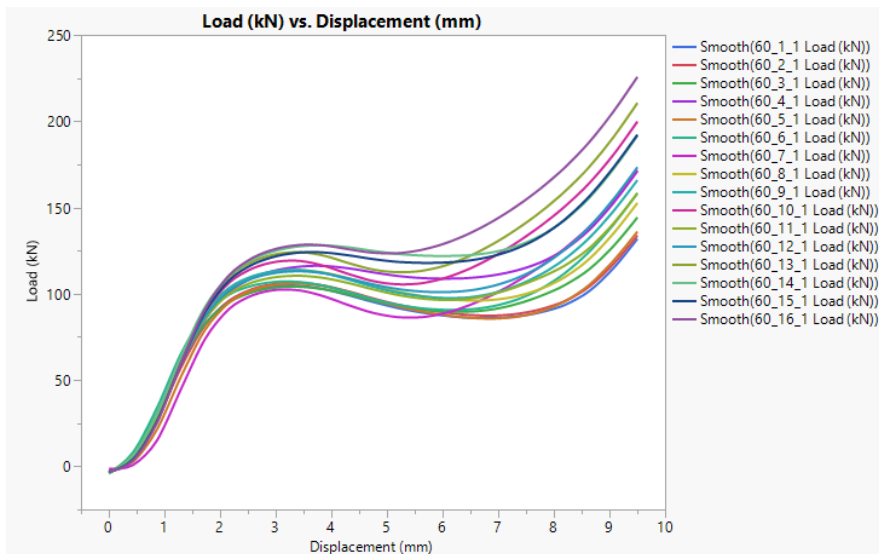


Figure 51: Load vs displacement data for 60-degree samples

After obtaining these load-displacement plots, they were normalized using bounding box section area and gauge length to compute stress and strain. Further, three mechanical properties were extracted to study their behavior function of the three varied geometric parameters defined in the sections above. The reported properties have all been normalized by mass and or volume to account for the fact that additional material was added to modify the geometry. Each mechanical property in relation to the three geometries is reported and analyzed independent of the others. Figure 52 shows the energy absorbed per unit mass, by each sample within this study.

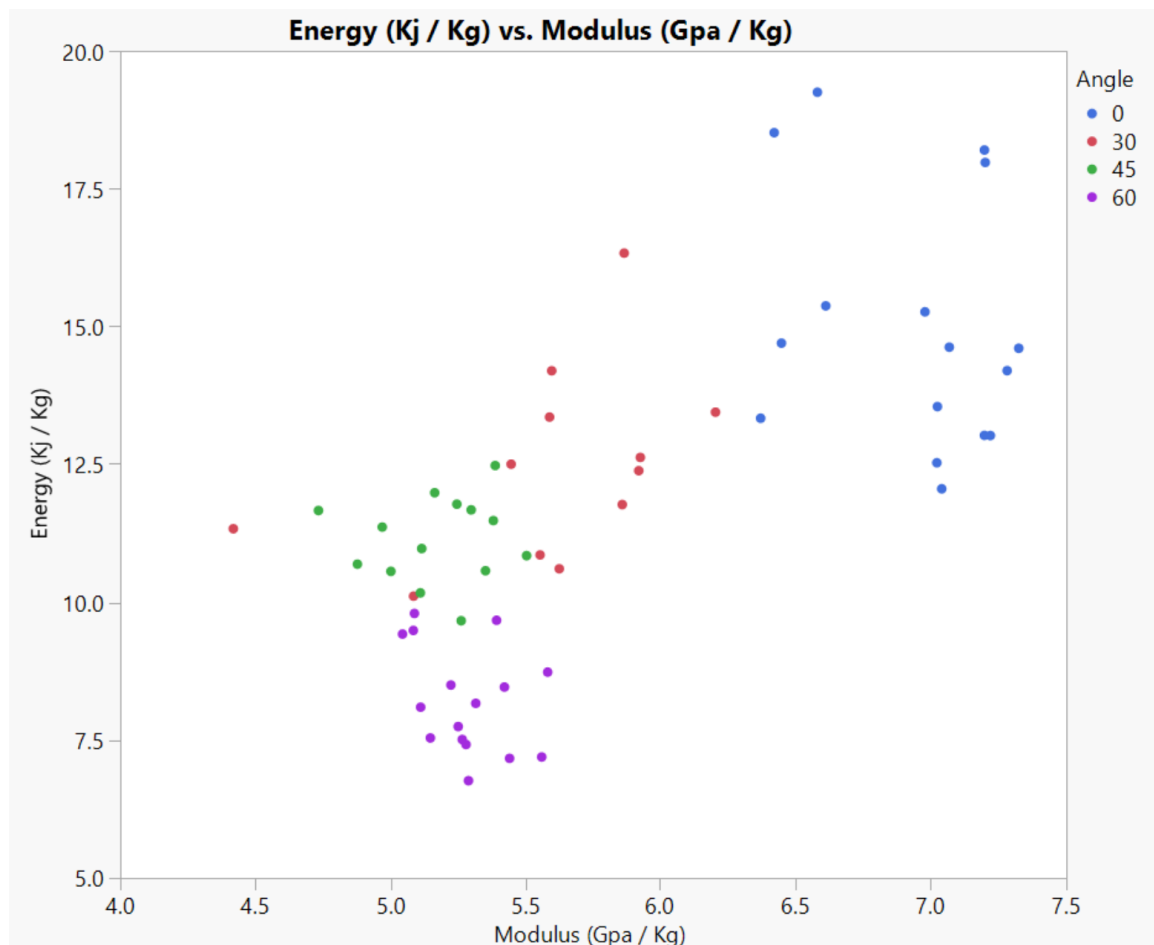
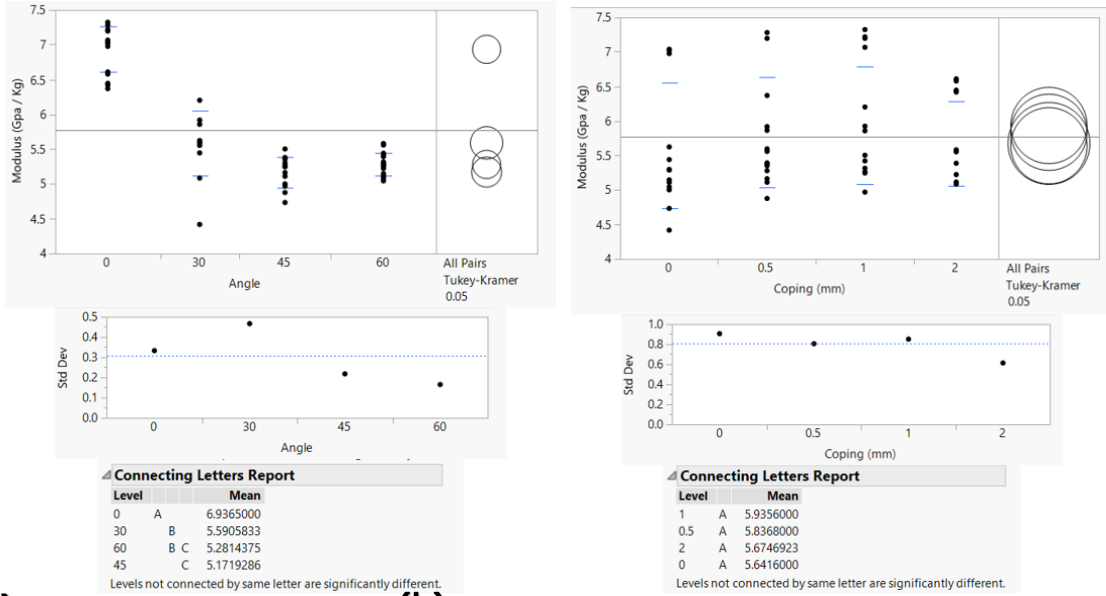


Figure 52: Energy density (per unit mass) versus specific modulus, with the interface angle color coded



(a)

(b)

(c)

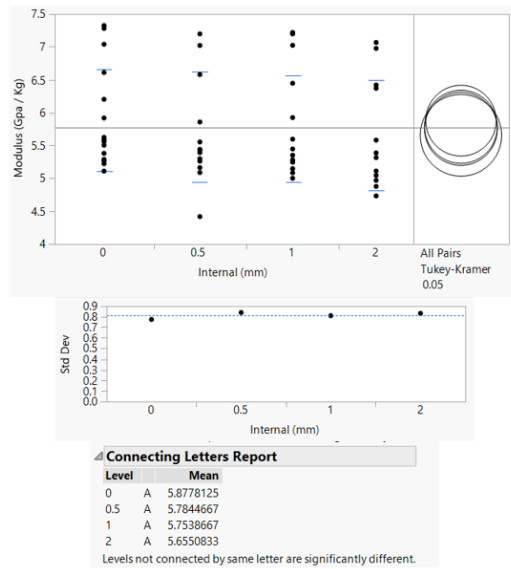


Figure 53: Modulus of elasticity plotted by (a) interface angle (b) Coping radius (c) internal radius

In Figure 53, it can be observed that as the angle of the internal interface increases, the modulus of the structure decreases. Within the variations of angle, no interface is statistically different from the others, 30-degree and 60-degree are statistically similar and 60-degree and 45-degree are statistically similar. It can also be observed for the internal and coping radius that all variations are statistically similar to each other.

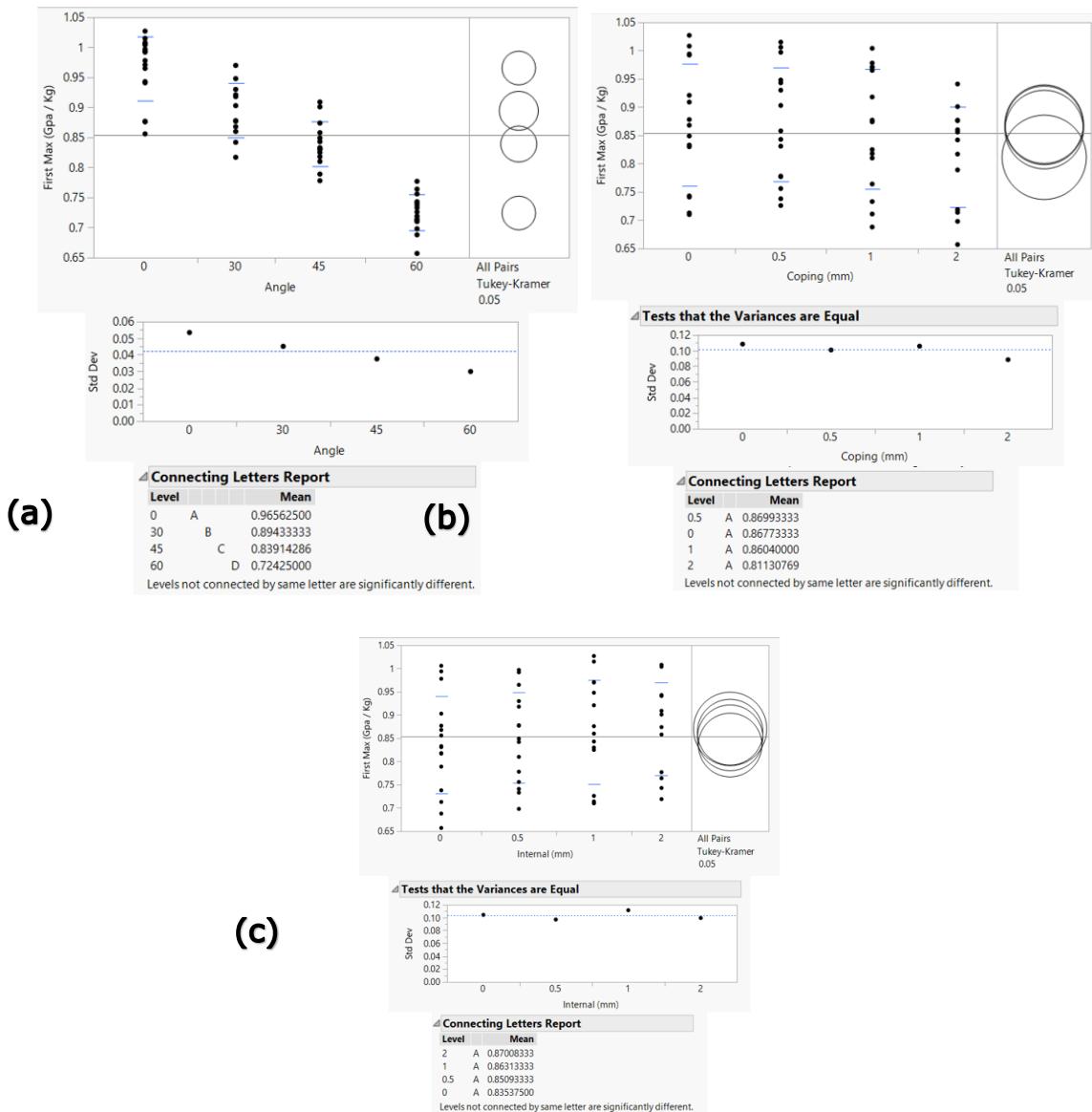


Figure 54: First maximum ultimate stress plotted by (a) interface angle (b) Coping radius (c) internal radius

In Figure 54, it can be observed that as the angle of the internal interface increases, the first maximum stress of the structure decreases. Within the variations of angle, each variation is statistically different from one another. It can also be observed for the internal and coping radius that all variations are statistically similar to each other.

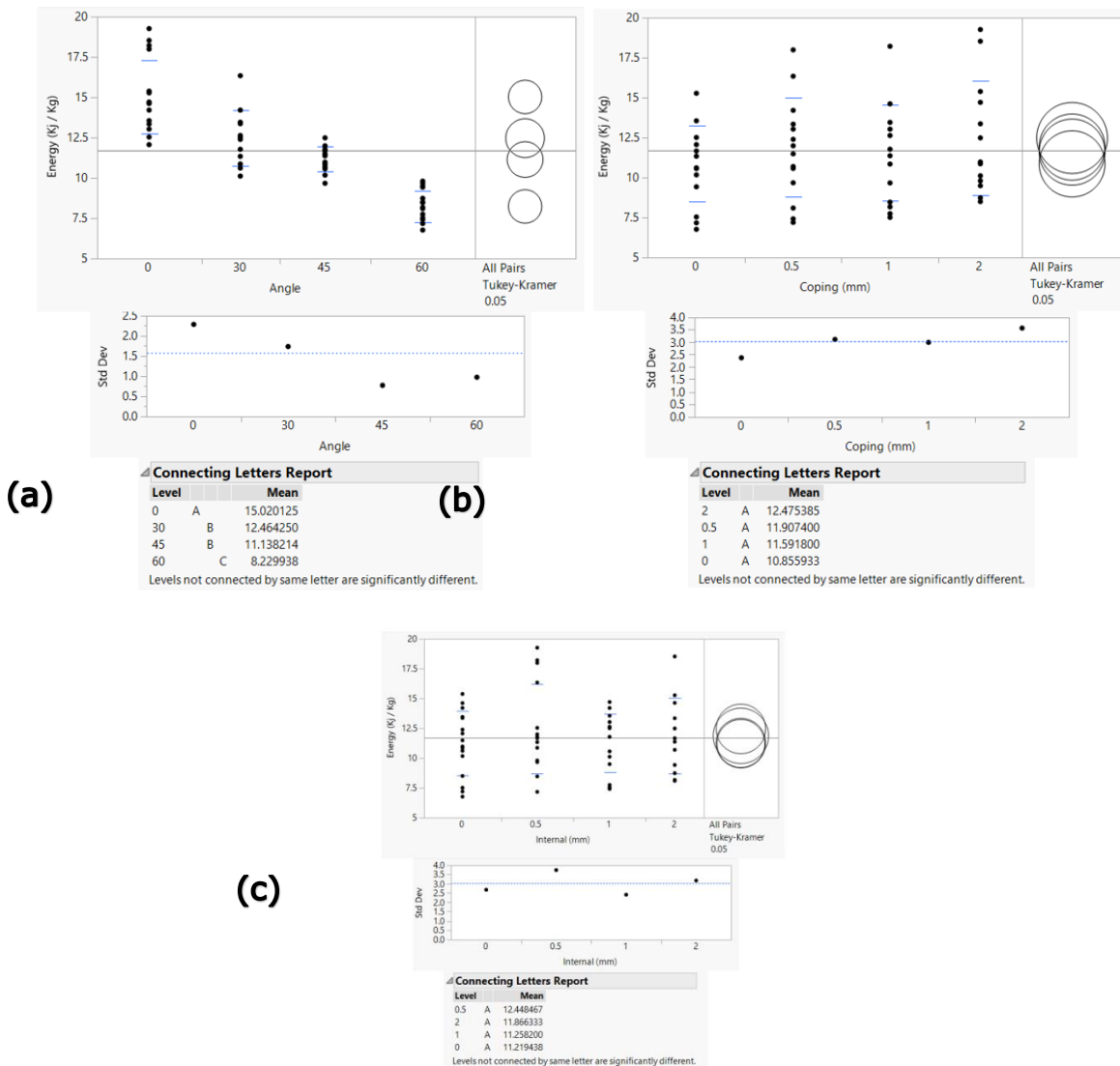


Figure 55: Energy absorbed plotted by (a) interface angle (b) Coping radius (c)

internal radius

In Figure 55, it can be observed that as the angle of the internal interface increases, the energy absorption of the structure decreases. Within the variations of angle, no interface is statistically different from the others, 30-degree and 45-degree are statistically similar and 45-degree and 60-degree are statistically similar. It can also be observed for the internal and coping radius that all variations are statistically similar to each other.

### 5.2.2 Three Point Bending

The following plots show calculated mechanical properties, flexural rigidity and flexural stress, by interface angle for all twelve samples. Both mechanical properties have been calculated using equations from ASTM D790 and normalized by mass, see Figure 59. There are only three samples per angle variation, these are not labeled because each of the samples are copies of the sample model. Future work for this analysis would be to print the full factorial variation of parameters and conduct more three-point bend testing.

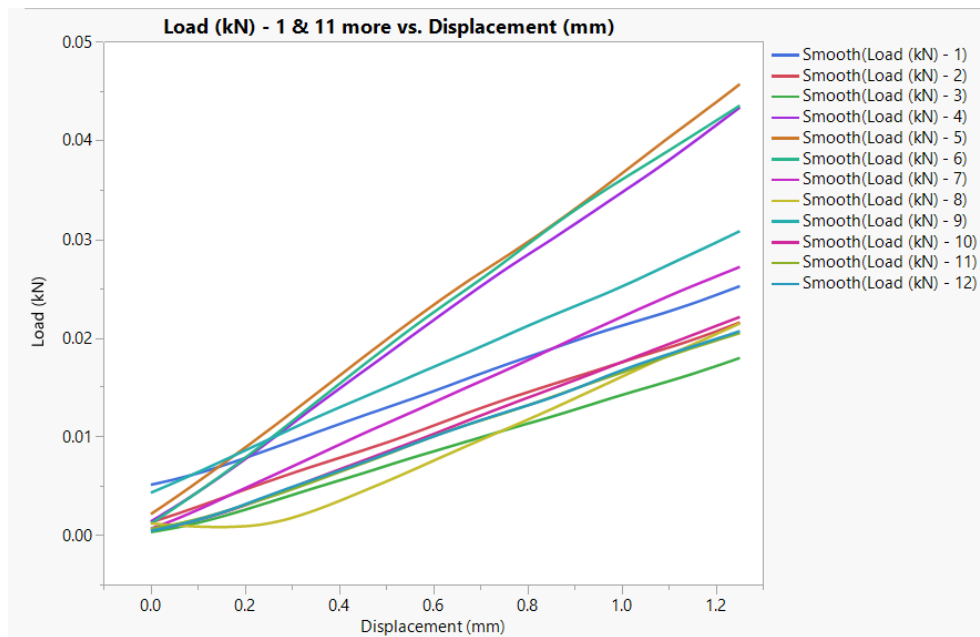


Figure 56: Three-point bend raw data

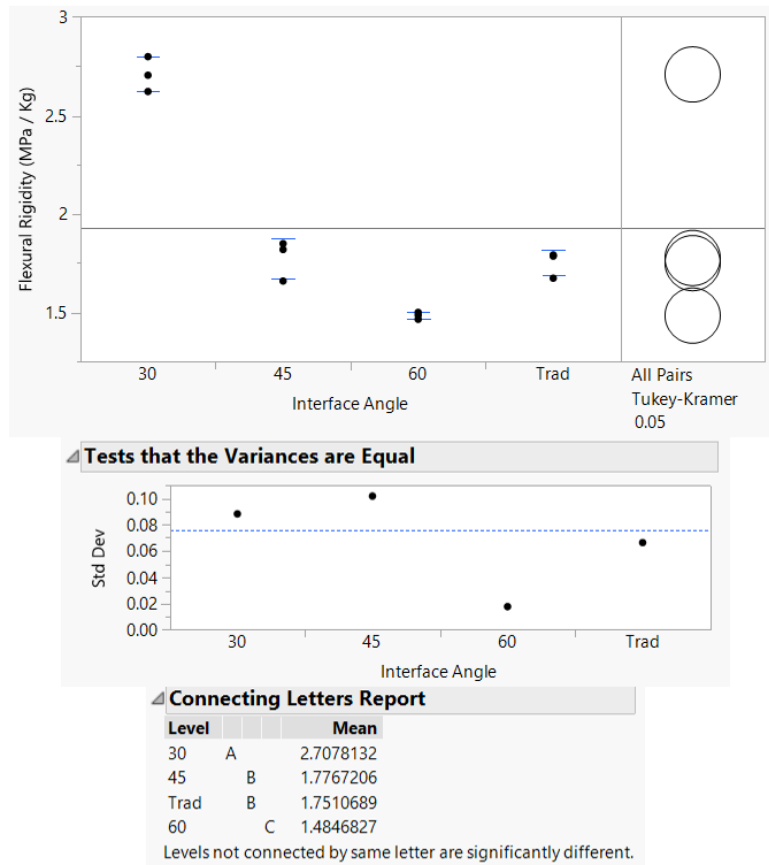


Figure 57: Flexural rigidity analysis

In Figure 57, it can be observed that as the angle of the internal interface increases, the flexural rigidity of the structure decreases. Within the variations of angle, 30-degree is statistically different from all other variations, 45-degree and no interface are statistically similar and 60-degree is statistically different from all other variations.

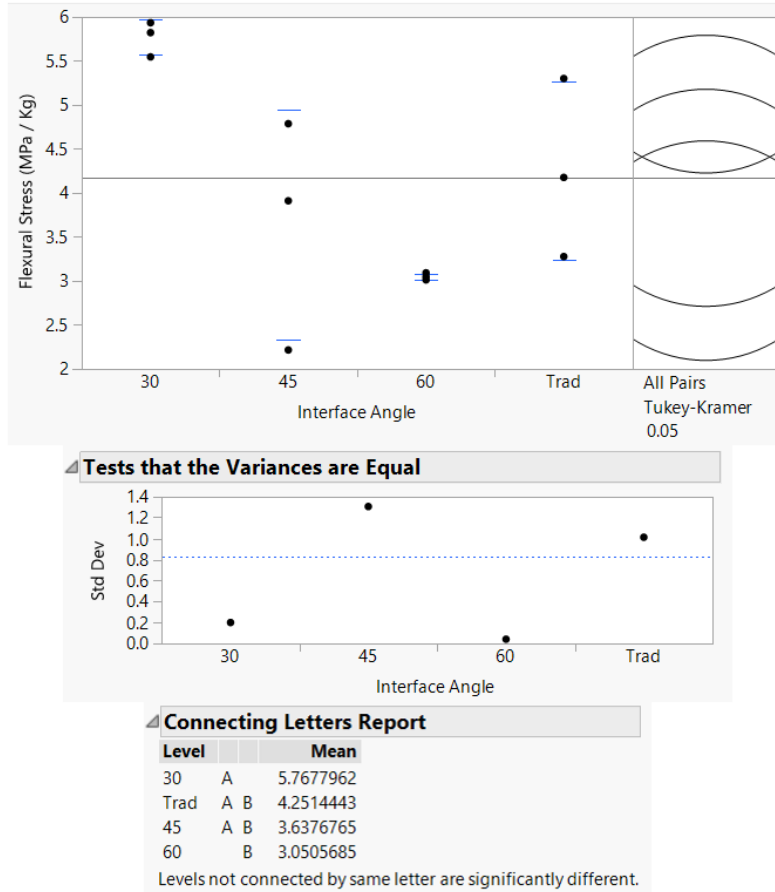


Figure 58: Maximum flexural stress analysis

In Figure 58, it can be observed that as the angle of the internal interface increases, the maximum flexural stress of the structure decreases. Within the variations of angle, 30-degree, no interface, and 45-degree are all statistically similar to one another while no interface, 45-degree and 60-degree are also statistically similar to one another.



12.2 *Flexural Stress ( $\sigma_f$ ):*

$$\sigma_f = 3PL/2bd^2 \quad (3)$$

where:

- $\sigma$  = stress in the outer fibers at midpoint, MPa (psi),
- $P$  = load at a given point on the load-deflection curve, N (lbf),
- $L$  = support span, mm (in.),
- $b$  = width of beam tested, mm (in.), and
- $d$  = depth of beam tested, mm (in.).

12.5.1 *Tangent Modulus of Elasticity:*

$$E_B = L^3m/4bd^3 \quad (6)$$

where:

- $E_B$  = modulus of elasticity in bending, MPa (psi),
- $L$  = support span, mm (in.),
- $b$  = width of beam tested, mm (in.),
- $d$  = depth of beam tested, mm (in.), and
- $m$  = slope of the tangent to the initial straight-line portion of the load-deflection curve, N/mm (lbf/in.) of deflection.

Figure 59: Equations used for three-point bend data

## CHAPTER 6

### CONCLUSIONS

This study has reported a comparative study of honeybee and wasp nest geometry and the biomimetic design of next generation honeycomb sandwich panels. Relations of geometric parameters within insect nest specimen were identified and investigated using statistical analysis. These parameters were then idealized and implemented into honeycomb sandwich panel core. These new core designs were then compared with traditional design to study how different parameter relations affect mechanical properties.

#### 6.1 Effect of Design Parameters

This section will summarize the findings and conclusions made for this study. The following section will discuss how this work should continue and what research can be done to further this study.

##### 6.1.1 Natural Specimens

This side of the study sought to examine how three geometric parameters, wall thickness, corner radius, and cell diameter related to one another within insect nests and if these relations were dependent on nest material. From data analysis of measurement taken from natural insect nests, the following conclusions have been drawn:

- Corner radius is a significant parameter that can be seen in all nests independent of material.
- With paper as the primary material, wall thickness and corner radius have a smaller ratio with cell diameter when compared to wax and mud nests.
- When normalized by cell diameter, corner radius and wall thickness are statistically similar independent of nest material.

### 6.1.2 Manufactured Specimens

This side of the study sought to examine how three geometric parameters, cell interface, internal radius and coping radius affected the mechanical behavior of honeycomb sandwich panel core compared to the traditional design. From the manufacturing and mechanical testing of these cores, the following conclusions have been made for compression cases:

- As the interface angle increases, the normalized mechanical properties of energy absorption, modulus of elasticity and ultimate stress decrease. Traditionally designed samples outperform all other variations of cell interface. This means adding this material and geometric complexity has no benefit to the overall performance of the structure.
- The addition and variation of both the internal and coping radius have no affect on the mechanical properties of the structure at this scale. As cells grow, ratios of these parameters to cell size may make a statistically significant difference but this was not seen in this study.

From the manufacturing and mechanical testing of these cores, the following conclusion has been made for three-point bend cases:

- Samples with a 30-degree cell interface outperform all other variations of this parameter with regard to flexural rigidity and flexural stress. Traditionally designed samples and those with a 45-degree interface outperform the 60-degree group. This leads to the conclusion that the steepest interface leads to the best mechanical performance.

### 6.2 Open Questions

This study chose to focus on structured white light microscopy for the bulk of data collection for the insect nest work while other methods such as Micro CT were only used for two scans. Structured blue light three-dimensional scanning was also

not used for any data collection. As stated above only one species of honeybee and wasp that used mud were examined during the course of this study. Only insects that produced hexagonal cells were studied, no other nesting type was parameterized or measured. Other examples of lattices, both periodic and aperiodic, exist in nature, none were observed during this study.

Compression and bend testing were conducted, mechanical testing of properties under tension and impact were not undertaken. Honeycomb core was designed, manufactured and tested, how these cores behave as part of a sandwich panel with facings was not studied. Each of the three main parameters had only four variations within the DOE. As stated previously, twelve bending samples were tested rather than the full DOE. Any multifunctionality of these structures hold was not observed.

## REFERENCES

- [1] J. F. V. Vincent, "Biomimetics - A review," *Proc. Inst. Mech. Eng. Part H J. Eng. Med.*, vol. 223, no. 8, pp. 919–939, 2009.
- [2] M. S. Aziz and A. Y. El Sherif, "Biomimicry as an approach for bio-inspired structure with the aid of computation," *Alexandria Eng. J.*, vol. 55, no. 1, pp. 707–714, 2016.
- [3] "Nature's Wisdom: 9 Brilliant Examples of Biomimicry in Design." [Online]. Available: <https://www.momtastic.com/webecoist/2014/12/31/natures-wisdom-9-brilliant-examples-of-biomimicry-in-design/>.
- [4] M. T. Varro, *Rerum Rusticarum Libri III.* .
- [5] T. C. Hales, "The honeycomb conjecture," *Discret. Comput. Geom.*, vol. 25, no. 1, pp. 1–22, 2001.
- [6] T. Rätz, "The silent hexagon: explaining comb structures," *Synthese*, vol. 194, no. 5, pp. 1703–1724, 2017.
- [7] Q. Zhang *et al.*, "Bioinspired engineering of honeycomb structure - Using nature to inspire human innovation," *Prog. Mater. Sci.*, vol. 74, pp. 332–400, 2015.
- [8] J. W. WENZEL, "A Generic key to the nests of hornets, yellowjackets, and paper wasps worldwide (Vespidae: Vespinae, Polistinae)," *Am. Museum Novit.*, vol. 3224, pp. 1–40, 1980.
- [9] B. P. Oldroyd and S. C. Pratt, *Comb Architecture of the Eusocial Bees Arises from Simple Rules Used During Cell Building*, 1st ed., vol. 49. Elsevier Ltd., 2015.
- [10] K. von Frisch, *Animal Architecture (English and German Edition)*, 1st ed. Harcourt, 1974.
- [11] H. R. Hepburn, C. W. W. Pirk, and O. Duangphakdee, *Honeybee Nests*, no. 1929. 2014.
- [12] "American Museum of Natural History." [Online]. Available: <https://www.viator.com/tours/New-York-City/American-Museum-of-Natural-History/d687-2396AMNH>. [Accessed: 04-Aug-2020].
- [13] "How does a micro-CT scanner work?" [Online]. Available: <https://www.microphotonics.com/how-does-a-microct-scanner-work/>. [Accessed: 02-Feb-2018].
- [14] E. Palermo, "What is Selective Laser Sintering?," 2013.